

# Neutrino masses and mixings

**Alessandro Strumia<sup>†</sup>**

*Theoretical Physics Division, CERN, CH-1211 Genève 23, Suisse*

**Francesco Vissani**

*INFN, Laboratori Nazionali del Gran Sasso, Theory Group, I-67010 Assergi (AQ), Italy*

## Abstract

After describing the general framework, the discoveries established in these years and some unconfirmed hints we outline few speculative experimental and theoretical ideas that could lead to the next developments.

We review the main experimental and theoretical issues related to neutrino masses and mixings. We try to present the physics in a simple way, avoiding unnecessary verbosity, formalisms and details. The bibliography does not contain all relevant works (authors will hopefully apologize). In order to avoid divagations we just refer to works that we believe can be useful to the reader. For example, we do not list papers whose content is already summarized in this review, that has no original content. When new developments will make it necessary, we will update the hep-ph/yymmnn version of this review, adding new sections or removing old ones, as listed below.

1. First version (yy/mm/2002). We would appreciate comments, criticisms, etc.

The review is structured as follows

- Section 1: a brief overview.
- Sections 2, 3, 4, 5: the basic tools.
- Sections 6, 7, 8: the established discoveries
- Sections 8, 9, 10: the missing discoveries, according to the simplest teorethical scheme.
- Section 11: unconfirmed anomalies.
- Sections 12, 10, 13, 14: possible lines of development.

Acronyms are explained in appendix A. Appendix B summarizes few basic facts concerning statistics.

# Contents

	7.5	Towards the final solution . . . . .	30
<b>1</b>	<b>Introduction</b>	<b>3</b>	<b>8</b>
1.1	Past . . . . .	3	<b>The global oscillation picture?</b>
1.2	Present . . . . .	4	31
1.3	Future? . . . . .	5	8.1 What remains to be done? . . . . .
<b>2</b>	<b>Neutrinos in the SM and beyond</b>	<b>5</b>	32
2.1	Extra fermion singlets . . . . .	7	<b>9</b>
2.2	Extra fermion triplets . . . . .	8	<b>Future oscillation experiments</b>
2.3	Extra scalar triplet . . . . .	8	32
<b>3</b>	<b>Majorana or Dirac neutrino masses</b>	<b>8</b>	9.1 Atmospheric experiments . . . . .
3.1	Pure Majorana neutrinos . . . . .	9	32
3.2	Pure Dirac neutrinos . . . . .	10	9.2 Solar experiments . . . . .
<b>4</b>	<b>Oscillations</b>	<b>11</b>	33
4.1	Oscillations in vacuum . . . . .	11	9.3 Reactor experiments . . . . .
4.2	Useful formulæ . . . . .	14	33
4.3	Oscillations in matter . . . . .	16	9.4 Neutrino beams . . . . .
4.4	Majorana vs Dirac neutrinos . . . . .	17	33
4.5	Oscillations in a varying density . . . . .	19	9.5 Superbeam . . . . .
<b>5</b>	<b>Detecting neutrinos</b>	<b>22</b>	33
5.1	Neutrino/electron scattering . . . . .	22	9.6 Neutrino factory . . . . .
5.2	Neutrino/nucleon scattering . . . . .	23	33
5.3	Neutrino/nucleus scattering . . . . .	25	<b>10</b>
<b>6</b>	<b>The atmospheric evidence</b>	<b>25</b>	<b>Non oscillation experiments</b>
6.1	Atmospheric neutrinos . . . . .	25	33
6.2	SuperKamiokande . . . . .	26	10.1 $\beta$ -decay . . . . .
6.3	Bounds from reactors . . . . .	28	33
6.4	Macro . . . . .	28	10.2 Neutrino-less double $\beta$ decay . . . . .
6.5	K2K . . . . .	28	34
<b>7</b>	<b>The solar evidence</b>	<b>28</b>	<b>11</b>
7.1	Solar neutrinos . . . . .	28	<b>Unconfirmed anomalies</b>
7.2	Fitting solar data . . . . .	30	34
7.3	Bounds from reactors . . . . .	30	11.1 LSND . . . . .
7.4	Non standard solar fits . . . . .	30	34
			11.2 NuTeV . . . . .
			35
			11.3 Heidelberg-Moscow . . . . .
			35
			11.4 Ultra-high energy cosmic rays . . . . .
			35
			<b>12</b>
			<b>Supernovæ</b>
			35
			12.1 What a supernova is . . . . .
			35
			12.2 Supernovæ and neutrinos . . . . .
			37
			12.3 Oscillations . . . . .
			38
			<b>13</b>
			<b>Understanding flavour</b>
			38
			13.1 Normal hierarchy . . . . .
			40
			<b>14</b>
			<b>Extras</b>
			40
			14.1 RGE effects . . . . .
			40
			14.2 Lepton-flavour violation from
			SUSY . . . . .
			40
			14.3 Connection with SUSY GUT . . . . .
			41
			14.4 Baryogenesis through leptogenesis . . . . .
			42
			<b>A</b>
			<b>Acronyms</b>
			43
			<b>B</b>
			<b>Statistics</b>
			43

# 1 Introduction

At the moment the solar and atmospheric anomalies are the only convincing evidences for new physics beyond the Standard Model. Still there is no direct experimental evidence that they are really due to neutrino oscillations with unexpectedly large mixing angles, rather than to some exotic mechanism. Neutrino physics is nowadays simpler than other less fruitful (so far) areas of physics: the main results do not require extensive MonteCarlo simulations, nor solving deep theoretical puzzles, nor experiments of G€ price performed by thousands of physicists. More importantly, neutrino experiments discovered something new, rather than giving only more precise measurements of SM parameters, or stronger bounds on unseen new physics.

Significant progress is expected in the next few years: the final solution of the solar and LSND anomalies, and long-baseline data about the atmospheric anomaly. If oscillations will be established, the so far unseen oscillation effects (the ‘third’ mixing angle and CP-violation) could be discovered soon or never, depending how large they are. Future data will also tell if ‘sterile neutrinos’  $\nu_s$  (i.e. extra light fermions with no gauge charge) have something to do with present anomalies, a possibility disfavoured by present data.

Before starting, we present a quick overview. We employ standard, usually self-explanatory notations, precisely defined in the next sections.

## 1.1 Past

After controversial results, in 1914 Chadwick established that the electrons emitted in radioactive  $\beta$  decays have a continuous spectrum, unlike what happens in  $\alpha$  [and  $\gamma$ ?] decays. It took some time to ensure that, if the  $\beta$  decay process were  ${}^A_ZX \rightarrow {}^A_{Z-1}Xe$  with only two particles in the final state, energy conservation would unavoidably imply a monochromatic electron spectrum.

On 4 december 1930 Pauli proposed a ‘desperate way out’ to save energy conservation, postulating the existence a new almost non-interacting particle, named “neutron”, with mass ‘of the same order of magnitude as the electron mass’ and maybe ‘penetrating power equal or ten times bigger than a  $\gamma$  ray’. The estimate of the cross-section was suggested by the old idea that particles emitted in radioactive decays were previously bound in the parent nucleus — rather than created in the decay process. In a 1934 [o 1933?] paper [1] containing ‘speculations too remote from reality’ (and therefore rejected by Nature) Fermi overcame this misconception and introduced a new length-scale (the ‘Fermi’ or ‘electroweak’ scale) in the context of a model able of predicting neutrino couplings in terms of  $\beta$ -decay lifetimes. Following a joke by Amaldi the new particle was renamed neutrino (in italian -one = big, -ino = small), when the true neutron was identified by Chadwick. Neutrinos were finally directly observed by Cowans and Reines in 1956 in a nuclear reactor experiment.

In those years  $K_0 \leftrightarrow \bar{K}_0$  effects were clarified, and this lead Pontecorvo to mention  $\nu \leftrightarrow \bar{\nu}$  oscillations in a 1957 paper. In 1962  $\nu_e \leftrightarrow \nu_\mu$  mixing was mentioned by Maki, Nakagawa and Sakata in the context of a wrong old-fashioned model of leptons bound inside hadrons. For these reasons some authors now name ‘MNS’ (or ‘MNSP’, or ‘PMNS’) the neutrino mixing matrix, although this is as improper as naming ‘indians’ the native habitants of America. The work that really lead to the first evidence for a neutrino anomaly, was done by Bahcall (that predicted the solar neutrino flux) and by Davis (that starting from 1968 measured a flux smaller than the predicted one). However, up to few years ago, it was not clear if there was a solar neutrino problem or a neutrino solar problem. Only recently experiments validated solar models and gave a strong evidence for a neutrino anomaly. Looking at the background of atmospheric neutrinos

the japanese (Super)Kamiokande experiment discovered a second  $\nu\tau$  anomaly.

## 1.2 Present

We have 2 established neutrino anomalies; so far there is no experimental evidence that they are really due to neutrino oscillations.

- The **atmospheric** evidence. SuperKamiokande observes disappearance of  $\nu_\mu$  and  $\bar{\nu}_\mu$  atmospheric neutrinos, with ‘infinite’ statistical significance ( $\sim 17\sigma$ ). If interpreted as oscillations, one needs  $\nu_\mu \rightarrow \nu_\tau$  with large mixing angle,  $\theta_{\text{atm}} \approx \pi/4$ , and with  $\Delta m_{\text{atm}}^2 \approx (1.5 \div 4) 10^{-3} \text{eV}^2$ . The other possibilities,  $\nu_\mu \rightarrow \nu_e$  and  $\nu_\mu \rightarrow \nu_s$ , cannot explain the anomaly and can only be present as small sub-dominant effects.
- The **solar** evidence. Various experiments see a  $\sim 50\%$  deficit of solar  $\nu_e$ . Combining all available experimental and theoretical ingredients, one gets a  $8\sigma$  solar anomaly. The NC and CC rates measured by SNO give a  $5\sigma$  direct evidence for  $\nu_e \rightarrow \nu_{\mu,\tau}$  (solar neutrinos have  $\sim \text{MeV}$  energy, so that experiments cannot distinguish  $\nu_\mu$  from  $\nu_\tau$ ). If interpreted as oscillations, one needs a large  $\theta_{\text{sun}} \lesssim \pi/4$  with  $10^{-5} \text{eV}^2 \lesssim \Delta m_{\text{sun}}^2 \lesssim 10^{-3} \text{eV}^2$  (‘LMA’ solution) or  $10^{-10} \text{eV}^2 \lesssim \Delta m_{\text{sun}}^2 \lesssim 10^{-6} \text{eV}^2$  (‘LOW’, ‘QVO’ solutions). Other oscillation interpretations in terms of a small mixing angle enhanced by matter effects, or in terms of sterile neutrinos, are now very strongly disfavoured.

Next, there are few unconfirmed anomalies

- **LSND** sees a  $(3 \div 7)\sigma$   $\bar{\nu}_\mu \rightarrow \bar{\nu}_e$  anomaly (the statistical significance varies depending how data are analyzed), maybe due to oscillations with  $\Delta m^2 \sim 1 \text{eV}^2$  and small mixing. Karmen has excluded part of the oscillation region suggested by LSND. A  $\bar{\nu}_\mu \rightarrow \bar{\nu}_s \rightarrow \bar{\nu}_e$  interpretation is disfavoured by other experiments.

The three possible oscillation effects (solar, atmospheric, LSND) require three different ranges of  $\Delta m^2$ . Therefore with oscillations of three neutrinos it is possible to fit only two anomalies. Usually one drops the LSND anomaly because it is the less solid one. In order to fit all anomalies, one can try to add one extra sterile neutrino. However this does not provide a satisfactory fit because none of the three anomalies is well fitted by sterile oscillations. If all three anomalies were true anomalies, it is likely that some unexpected new physics is involved.

- **NuTeV** claims a  $3\sigma$  anomaly in neutrino *couplings*: the measured ratio between the  $\nu_\mu$ /iron NC and CC couplings is about 1% lower than some SM prediction. Specific QCD effects that cannot be computed in a reliable way could be the origin of the NuTeV anomaly.
- A reanalysis of the **Heidelberg-Moscow** data claims a  $(2.2 \div 3)\sigma$  hint for violation of lepton number. The simplest interpretation would be in terms of Majorana neutrino masses, implying approximatively degenerate neutrinos with mass  $m \sim 0.4 \text{eV}$ . In our opinion these data do not contain a statistically significant hint:  $1.5\sigma$  at most.
- CHORUS

Furthermore, there are some important constraints

---

<sup>1</sup>‘Nyu tori no’ i.e. neutrino doubly distorted due to limitations of hiragana (to) and english (nyu) phonetics.

- LEP data tell that there are only 3 neutrinos (but other light fermions with no gauge interactions might exist, and could play the rôle of ‘sterile neutrinos’).
- CHOOZ constrains  $\bar{\nu}_e$  disappearance effects at the atmospheric frequency to be smaller than few %.
- Beta and double-beta decay searches imply that neutrinos are lighter than about 1 eV.

### 1.3 Future?

Important progress is expected in the next few years:

2002 **KamLAND** will definitively test the LMA solution (maybe already knows the answer)

2003 **Borexino** and maybe KamLAND begin to test the other solutions of the solar anomaly, and **MiniBoone** tests the LSND anomaly.

2005 3 **long-baseline** experiments (Minos, CNGS and the already running K2K) will better measure the atmospheric parameters, and maybe discover  $\theta_{13}$  (i.e.  $\nu_\mu \rightarrow \nu_e$  oscillations at the atmospheric frequency).

200? Some big **neutrino-less double-beta decay** experiment will search for violation of lepton number (e.g. Majorana  $\nu$  masses). Some experiment could confirm the solar anomaly looking at **sub-MeV solar neutrinos**. Nobel prize for SK.

2008 **LHC** begins to explore physics above the electroweak scale; maybe having some indirect relevant impact on neutrino physics.

2010 **JHF**. Around 2007 an intense low-energy  $\nu_\mu$  beam will be sent to SK. There are plans to upgrade the beam and the detector. Hopefully, a HyperKamiokande experiment with a Mton of water can search for  $p$ -decay, for  $\theta_{13}$  and CP-violation in neutrino oscillations.

2020 Sooner or later a **neutrino factory** will perform the ‘ultimate’ search for these oscillations effects and for lepton-flavour violating  $\mu$  decays. Neutrino couplings will also be tested.

2030 december 4:  $\nu$  centennial. This is the only safe expectation.

## 2 Neutrinos in the SM and beyond

In all observed processes baryon and lepton number are conserved. This is nicely explained within the SM: the most general gauge-invariant renormalizable Lagrangian that can be written with the SM fields (the Higgs  $H$  doublet, the lepton doublets  $L = (\nu_L, \ell_L)$ , the lepton singlets  $E = \ell_R$ , etc) beyond ‘minimal’ terms (kinetic and gauge interactions) can only contain the following Yukawa and Higgs-potential terms

$$\mathcal{L}_{\text{SM}} = \mathcal{L}_{\text{minimal}} + \lambda_E ELH^* + \lambda_D DQH^* + \lambda_U UQH + m^2|H^2| - \lambda|H|^4.$$

(hermitian conjugates are left understood). No term violates baryon number  $B$  and lepton flavour  $L_e, L_\mu, L_\tau$  (as well as lepton number  $L = L_e + L_\mu + L_\tau$ ), that therefore naturally emerge as *accidental* symmetries. Baryon flavour and CP are violated in a very specific way, that implies (among other things) very small electric dipoles and a characteristic rate of  $K_0 \leftrightarrow \bar{K}_0$  transitions.

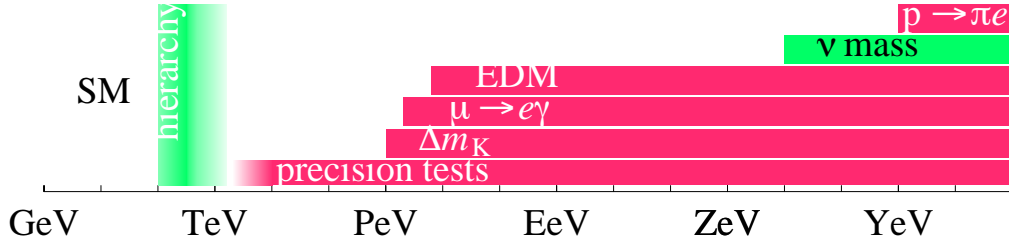


Figure 1: *Bounds on the scale  $\Lambda$  that suppresses non-renormalizable operators that violate  $B, L, CP, L_f, B_f$  and affect precision data. Maybe the ‘hierarchy problem’ suggests new-physics around few hundred GeV.*

When the Higgs takes its vev  $\langle H \rangle = (0, v)$  with  $v \approx 174$  GeV, charged leptons and quarks get Dirac<sup>2</sup> mass terms  $m_i = \lambda_i v$

$$m_E \ell_R \ell_L + m_D d_R d_L + m_U u_R u_L$$

but neutrinos remain massless. Within the SM, neutrinos are fully described by the Lagrangian term

$$\bar{L} i \not{D} L$$

i.e. a kinetic term, plus gauge interactions with the massive vector bosons,  $\bar{\nu} Z \nu$  and  $\bar{\nu} W \ell_L$ .

Massive neutrinos require some extension of the SM.

The new physics can be either lighter or heavier than the maximal energy that have so far experimentally explored, around 100 GeV.

In the first case, one can add light right-handed neutrinos  $\nu_R$ , and obtain Dirac neutrino masses from the additional Yukawa term  $\lambda_N \nu_R L H$ .  $m_\nu = \lambda_N v \approx 0.1$  eV for  $\lambda_N \sim 10^{-12}$ .

Alternatively, generic new physics too heavy for being directly studied manifests at low energy as non renormalizable operators (NRO), suppressed by heavy scales  $\Lambda$ . NRO have little effect on low energy processes, that are dominated by renormalizable operators. Particularly interesting are those small effects that cannot be generated by renormalizable operators. When NRO are added to the SM Lagrangian,  $L_e, L_\mu, L_\tau, B$  are no longer accidentally conserved:

$$\mathcal{L} = \mathcal{L}_{\text{SM}} + \frac{1}{\Lambda_L} (LH)^2 + \frac{1}{\Lambda_B^2} QQQ L + \dots$$

<sup>2</sup>Dirac and Majorana quadri-spinors are usually presented following the historical development and notation, but this is confusing. Quadri-spinors are representations of the Lorentz group and of parity, that was believed to be an exact symmetry. Since we now know that this is not the case, it is more convenient to use the basic fermion representations of the Lorentz group: the 2-dimensional Weyl spinors. The only Lorentz invariant mass term that can be written with a single Weyl fermion  $\psi$  is the Majorana term  $\psi^2$ . This mass term breaks a U(1) symmetry  $\psi \rightarrow e^{iq_\psi \varphi} \psi$  under which  $\psi$  might be charged (it could be electric charge, lepton number, ...). With two Weyl fermions  $\psi$  and  $\psi'$  one can write three mass terms:  $\psi^2$ ,  $\psi'^2$  and  $\psi\psi'$ . In many interesting cases (all SM fermions, except maybe neutrinos) the Lagrangian has an unbroken U(1) symmetry (electromagnetism, in the SM) under which  $\psi$  and  $\psi'$  have opposite charges, so that then  $\psi\psi'$  is the only allowed mass term. It is named ‘Dirac mass term’, and one can group  $\psi$  and  $\psi'$  in one 4-component Dirac spinor  $\Psi = (\psi, \bar{\psi}')$ . The electron gets its mass from a Dirac term, that joins two different Weyl fermions that are therefore named  $e_L$  and  $e_R$  rather than  $\psi$  and  $\psi'$ . If one knows what is doing this is the simplest notation. Since  $e_L$  and  $e_R$  have opposite electric charges one usually prefers to use names like ‘ $\bar{e}_R$ ’ or ‘ $e_R^c$ ’ in place of ‘ $e_R$ ’ but this causes confusion when over-bars or charge-conjugates are needed for other reasons.



The dimension-5 operator  $(LH)^2$  gives a Majorana neutrino mass term,  $m_\nu \nu_L^2$ , with  $m_\nu \sim v^2/\Lambda_L \sim 0.1 \text{ eV}$  for  $\Lambda_L \sim 10^{14 \div 15} \text{ GeV}$ . Neutrino masses might be the first manifestation for a new length scale in nature, similarly to what happened when the 1896 discovery of radioactivity by Becquerel later lead Fermi to add non renormalizable operators suppressed by the electroweak scale.

The dimension-6 operator  $QQQL$  gives rise to proton decay. Furthermore, other operators give additional sources of CP and hadronic flavour violation, or affect precision LEP data. Except neutrino masses, none of these effects have been observed, and the strongest bounds are summarized in fig. 1.

It is interesting to speculate about which renormalizable extensions of the SM can generate neutrino masses. One needs to add some new particle. Even taking into account that LEP excluded new particles coupled to the  $Z$  boson and lighter than  $M_Z/2$ , there are still 3 simple allowed possibilities, and many less simple possibilities.

## 2.1 Extra fermion singlets and ‘see-saw’

The simplest possibility is adding new fermions with no gauge interactions, that play the rôle of ‘right-handed neutrinos’,  $N = \nu_R$ . If they exist, one can add to the SM Lagrangian two extra renormalizable terms

$$\mathcal{L} = \mathcal{L}_{\text{SM}} + \lambda_N NLH + \frac{M_N}{2} N^2 \quad \text{giving the } 6 \times 6 \text{ mass matrix} \quad \begin{array}{cc} & \begin{array}{c} \nu_L \\ \nu_R \end{array} \\ \begin{array}{c} \nu_L \\ \nu_R \end{array} & \begin{pmatrix} 0 & \boldsymbol{\lambda}_N^T v \\ \boldsymbol{\lambda}_N v & \mathbf{M}_N \end{pmatrix} \end{array}$$

where bold-face reminds that  $\boldsymbol{\lambda}_N$  and  $\mathbf{M}_N$  are  $3 \times 3$  flavour matrices. The values of  $\lambda_N$  and  $M_N$  could be related to the unification scale, or to supersymmetry-breaking or to the size of extra dimensions or to some other ‘fundamental’ physics, but in practice we do not know. We focus on two interesting extreme limits:

- **Pure Majorana neutrinos:** if  $M_N \gg \lambda_N v$  the full  $6 \times 6$  mass matrix gives rise to 3 (almost) pure right-handed neutrinos with heavy Majorana masses  $\mathbf{M}_N$ , and to 3 (almost) pure left-handed neutrinos with light Majorana masses  $\mathbf{m}_\nu = -(v\boldsymbol{\lambda}_N)^T \mathbf{M}_N^{-1} (v\boldsymbol{\lambda}_N)$ .

We now rederive the same result proceeding in a different way. Integrating out the heavy neutrinos gives a non-renormalizable effective Lagrangian that only contains the observable low-energy fields. Fig. 2a shows that  $\nu_R$  exchange generates the Majorana mass operator  $(LH)^2$  with coefficient  $-\boldsymbol{\lambda}_N^T \mathbf{M}_N^{-1} \boldsymbol{\lambda}_N$ .

This ‘see-saw’ mechanism works naturally and fits nicely in grand unified extension of the SM. It generates the 9 measurable neutrino parameters (see section 3) from  $\boldsymbol{\lambda}_N$  and  $\mathbf{M}_N$ , that contain 18 unknown parameters. Still, it might be not impossible to test it experimentally (section 14).

- **Pure Dirac neutrinos:** if  $M_N \ll \lambda_N v$  the full  $6 \times 6$  mass matrix gives 3 Dirac neutrinos  $\Psi = (\nu_L, \bar{\nu}_R)$  with mass  $m_\nu = \lambda_N v$ . The vanishing of  $M_N$  can be justified if conservation of lepton number is *imposed* (rather than obtained, as in the SM). In order to get the observed neutrino masses one needs  $\lambda_\nu \sim 10^{-13}$  — much smaller than all other SM Yukawa couplings.

More generically, one could have  $M_N \sim v$  (giving light Majorana neutrinos) or  $M_N \sim \lambda_N v$  (giving 6 mixed neutrinos with comparable masses).

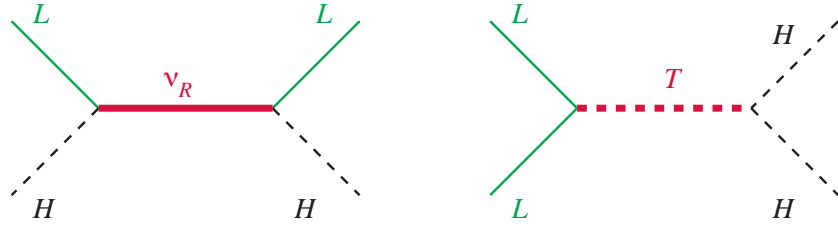


Figure 2: *Neutrino masses generated by (a) a neutral fermion (‘see-saw’) (b) a scalar triplet.*



Figure 3: *Possible neutrino spectra: (a) normal (b) inverted.*

## 2.2 Extra fermion triplets

The extra fermion  $N$  added in the previous section could be a  $SU(2)_L$  triplet, rather than a singlet. One has analogous  $\lambda_N$  and  $M_N$  flavour matrices. As long as  $M_N \gg v$  (triplets lighter than  $M_Z/2$  have been excluded by LEP) everything works in the same way: triplet exchange generates the Majorana mass operator,  $(LH)^2$ .

## 2.3 Extra scalar triplet

Alternatively, one can add one *scalar* triplet  $T$  with appropriate hypercharge, such that the most generic renormalizable Lagrangian is

$$\mathcal{L} = \mathcal{L}_{\text{SM}} + \lambda_T L L T + \frac{M_T}{2} |T|^2 + m H H T^*.$$

Integrating out the heavy triplet generates the Majorana neutrino masses operator  $(LH)^2$  (see fig. 2b) with coefficient  $\propto \lambda_T m / M_T^2$ , where  $\lambda_T$  is a flavour matrix. A smaller number of unknown flavour parameters are needed to describe one extra scalar triplet than the extra fermion scalars or triplets.

Finally, one may also imagine more complicated possibilities. For example, one could add extra particles  $A, B$  with couplings of the form  $LAB$  and  $HAB$  (we do not list all the possibilities), so that exchanging  $A$  and  $B$  generates the  $(LH)^2$  operator at one loop.

## 3 Majorana or Dirac neutrino masses

We now study in detail the special cases of pure Majorana and Dirac neutrino masses. We describe how many and which parameters can be measured in the two cases by low energy experiments.



### 3.1 Pure Majorana neutrinos

We extend the SM by adding to its Lagrangian the non-renormalizable operator  $(LH)^2$  and no new fields. Below the  $SU(2)_L$ -breaking scale,  $(LH)^2$  just gives rise to Majorana neutrino masses. In this situation, charged lepton masses are described as usual by a complex  $3 \times 3$  matrix  $\mathbf{m}_E$ , and neutrino masses by a complex symmetric  $3 \times 3$  matrix  $\mathbf{m}_\nu$ :

$$-\mathcal{L}_{\text{mass}} = \ell_R^T \cdot \mathbf{m}_E \cdot \ell_L + \frac{1}{2} \nu_L^T \cdot \mathbf{m}_\nu \cdot \nu_L.$$

How many independent parameters do they contain? Performing the usual unitary flavour rotations of right-handed  $E = \ell_R$  and left-handed  $L = (\nu_L, \ell)$  leptons, that do not affect the rest of the Lagrangian,<sup>3</sup> we reach the standard mass eigenstate basis of charged leptons, where  $m_E = \text{diag}(m_e, m_\mu, m_\tau)$ . It is still possible to redefine the phases of  $e_L$  and  $e_R$  such that  $m_e$  and  $m_\nu^{ee}$  are real and positive; and similarly for  $\mu$  and  $\tau$ . Therefore charged lepton masses are specified by 9 real parameters and 3 complex phases: the 3 real parameters  $m_e, m_\mu, m_\tau$ ; the 3 real diagonal elements of  $m_\nu$ ; the 3 complex off-diagonal elements of  $m_\nu$ .

It is customary to write the mass matrices as

$$m_E = \text{diag}(m_e, m_\mu, m_\tau), \quad m_\nu = V^* \text{diag}(m_1 e^{-2i\beta}, m_2 e^{-2i\alpha}, m_3) V^\dagger \quad (1)$$

where  $m_{e,\mu,\tau,1,2,3} \geq 0$ . The neutrino mixing matrix  $V$  (that relates the neutrinos with given mass,  $\nu_i$ , to those with given flavour,  $\nu_\ell = V_{\ell i} \nu_i$ ) can be written as

$$V = R_{23}(\theta_{23}) \cdot \text{diag}(1, e^{i\phi}, 1) \cdot R_{13}(\theta_{13}) \cdot R_{12}(\theta_{12}) \quad (2)$$

where  $R_{ij}(\theta_{ij})$  represents a rotation by  $\theta_{ij}$  in the  $ij$  plane and  $i, j = \{1, 2, 3\}$ . In components

$$\begin{pmatrix} V_{e1} & V_{e2} & V_{e3} \\ V_{\mu 1} & V_{\mu 2} & V_{\mu 3} \\ V_{\tau 1} & V_{\tau 2} & V_{\tau 3} \end{pmatrix} = \begin{pmatrix} c_{12}c_{13} & c_{13}s_{12} & s_{13} \\ -c_{23}s_{12}e^{i\phi} - c_{12}s_{13}s_{23} & c_{12}c_{23}e^{i\phi} - s_{12}s_{13}s_{23} & c_{13}s_{23} \\ s_{23}s_{12}e^{i\phi} - c_{12}c_{23}s_{13} & -c_{12}s_{23}e^{i\phi} - c_{23}s_{12}s_{13} & c_{13}c_{23} \end{pmatrix}. \quad (3)$$

Within this standard parameterization, the 6+3 neutrino parameters are the 3 neutrino mass eigenvalues,  $m_1, m_2, m_3$ , the 3 mixing angles  $\theta_{ij}$  and the 3 CP-violating phases  $\phi, \alpha$  and  $\beta$ .  $\phi$  is the analogous of the CKM phase.  $\alpha$  and  $\beta$  are called ‘Majorana phases’ and do not affect oscillations (see section 4).

We now justify this parameterization.

1. Two parameters,  $\theta_{23}$  and  $\theta_{13}$ , are necessary to describe the flavour of the most splitted neutrino mass eigenstate

$$|\nu_3\rangle = s_{13}|\nu_e\rangle + c_{13}s_{23}|\nu_\mu\rangle + c_{13}c_{23}|\nu_\tau\rangle.$$

Complex phases can be rotated away by redefining the phases of  $L_{e,\mu,\tau}$  and  $E_{e,\mu,\tau}$  leaving  $m_{e,\mu,\tau}$  real and positive. Physically, this means that *two* mixing angles,  $\theta_{23}$  and  $\theta_{13}$ , give rise to CP-conserving oscillations at the larger frequency  $\Delta m_{23}^2$ .

2. Since the flavours of  $|\nu_2\rangle$  and  $|\nu_3\rangle$  must be orthogonal, a single complex mixing angle (decomposed as one real mixing angle,  $\theta_{12}$ , plus one relative phase,  $\phi$ ) are needed to describe the flavour of  $|\nu_2\rangle = \sum_\ell V_{\ell 2}^* |\nu_\ell\rangle$ . Since there is no longer any freedom to redefine the phases of  $\nu_{e,\mu,\tau}$ , the overall phase of  $|\nu_2\rangle$ ,  $\alpha$ , is physical.

---

<sup>3</sup>Gauge interactions are the same in any flavour basis, because kinetic energy and gauge interaction originate from the same Lagrangian term,  $\bar{L}\not{D}L$ . This non-trivial fact rests on solid experimental and theoretical grounds. The story would be different if neutrinos had extra interactions.

3. Finally, no more parameters are needed to describe the flavour of  $\nu_1$ , that must be orthogonal to  $\nu_2$  and  $\nu_3$ . The overall phase of  $\nu_1$ ,  $\beta$ , cannot be rotated away and is a physical parameter.

Finally, we specify the full allowed range of the parameters.

We order the neutrino masses  $m_i$  such that  $m_3$  is the most splitted state and  $m_2 > m_1$ , and define  $\Delta m_{ij}^2 = m_j^2 - m_i^2$ . With this choice,  $\Delta m_{23}^2$  and  $\theta_{23}$  are the ‘atmospheric parameters’ and  $\Delta m_{12}^2 > 0$  and  $\theta_{12}$  are the ‘solar parameters’, whatever the spectrum of neutrinos (‘normal hierarchy’ so that  $\Delta m_{23}^2 > 0$ ; or ‘inverted hierarchy’ so that  $\Delta m_{23}^2 < 0$ , see fig. 3). With this choice the physically inequivalent range of mixing angles is

$$0 \leq \theta_{12}, \theta_{23}, \theta_{13} \leq \pi/2, \quad 0 \leq \phi < 2\pi \quad 0 \leq \alpha, \beta < 2\pi???$$

The flavour composition of the neutrino mass eigenstates  $\nu_{1,2,3}$  suggested by present data is indicated in fig. 3 in a self-explanatory pictorial way.

### 3.2 Pure Dirac neutrinos

We extend the SM by adding three neutral singlets (one per family), named “right-handed neutrinos”,  $\nu_R$ . We forbid  $\nu_R^2$  mass terms by imposing conservation of lepton number (or of its anomaly-free cousin  $B - L$ ). The most generic renormalizable Lagrangian contains the additional term

$$\mathcal{L} = \mathcal{L}_{\text{SM}} + \lambda_N \nu_R L H.$$

In this situation, charged lepton masses are described as usual by a complex  $3 \times 3$  matrix  $\mathbf{m}_E$ , and neutrino masses by a complex  $3 \times 3$  matrix  $\mathbf{m}_\nu = \boldsymbol{\lambda}_N v$ :

$$-\mathcal{L}_{\text{mass}} = \ell_R^T \cdot \mathbf{m}_E \cdot \ell_L + \nu_R^T \cdot \mathbf{m}_\nu \cdot \nu_L$$

How many physical parameters do they contain? We have more matrix elements and more fields that can be rotated than in the pure Majorana case. One can repeat the steps 1, 2, 3 above, with the only modification that the ‘Majorana phases’ can now be rotated away (reabsorbed in the phases of the  $\nu_R$ ) leaving only the CKM phase.

In fact, the flavour structure (2 mass matrices for 3 kinds of fields) is identical to the well known structure present in quarks (2 mass matrices for the up and down-type quarks, contained in the 3 fields  $u_R$ ,  $d_R$  and  $Q = (u_L, d_L)$ ). However, a numerical difference makes the physics very different: neutrino masses are small. Up and down-type quarks and charged leptons are produced in ordinary processes as mass eigenstates, while neutrinos as flavour eigenstates. So far, we can produce a  $\nu_\mu$ , but we are not able of getting a  $\nu_3$ . For this reason, tools like ‘unitarity triangles’ have no practical use in lepton flavour — other presentations are more appropriate.

Before concluding, let us discuss the physical difference between Majorana and Dirac neutrinos.

To begin, let us consider an imaginary experiment. Suppose that it would be possible to put at rest a massive  $\nu_\mu$  neutrino with spin-down in the middle of the room. If accelerated up to relativistic energies in the up direction, when it hits the roof can produce a  $\mu^-$  trough a CC interaction. If accelerated up to relativistic energies in the down direction, when it hits the floor it can produce a  $\mu^+$  (if it is a Majorana particle) or have no interaction (if it is a Dirac particle).

Coming to realistic experiments, in the next section we show that oscillation experiments cannot discriminate Majorana from Dirac neutrinos. No signal induced by neutrino masses other than oscillations has so far been seen. It seems that the only realistic hope of experimentally discriminating Majorana from Dirac neutrino masses is based on the fact that Majorana masses violate lepton number, maybe giving a signal in future neutrino-less double  $\beta$  decay searches (section 10.2).

## 4 Oscillations

We first discuss vacuum oscillations. Before giving practical formulæ, following [?] we discuss the subtle points hidden in the standard oversimplified derivation. Next, we discuss oscillations in matter, and describe how neutrinos oscillate in the sun.

### 4.1 Oscillations in vacuum

One-particle quantum mechanics is the appropriate language for describing neutrino oscillations. In all cases of practical interest neutrino fluxes are sufficiently weak that multi-particle Fermi-Dirac effects can be neglected. Concerning this aspect, a neutrino beam is simpler than an electro-magnetic field, that can be composed by inequivalent configurations of many photons. Therefore, one should

1. **Build a neutrino wave-packet**, taking into account the dynamics of the specific process that produces it, For example, atmospheric and beam neutrinos are mostly produced in  $\pi$  and  $\mu$  decays. Solar  $\nu_e$  are produced in collisions and decays of light nuclei inside the sun. Reactor  $\bar{\nu}_e$  by slow decays of heavy radioactive nuclei. Supernova neutrinos are produced thermally.
2. **Study its evolution.** Different mass eigenstates acquire different phases, giving rise to oscillations. The mass difference also generates other effects. The lighter mass eigenstate moves faster than the heavier one: at some point their wavepackets no longer overlap, destroying oscillations. While in neutrinos this effect is usually negligible, the mass differences between quarks are so large that there are no oscillations between quarks: e.g. the down-type quark  $q$  produced in decays of charmed hadrons,  $c \rightarrow q\ell\bar{\nu}$ , is  $|q\rangle = \cos\theta_C|d\rangle + \sin\theta_C|s\rangle$ , giving rise to a  $\pi$  with probability  $\cos^2\theta_C$  and to  $K$  with probability  $\sin^2\theta_C$  — not to  $\pi \leftrightarrow K$  oscillations. (Furthermore the heavier quarks decay fastly, while the heavier neutrinos probably do not).
3. **Compute the observable to be measured**, taking into account what the detector is really doing. Oscillations are a quantum interference effect. The necessary coherence is destroyed if the neutrino mass is measured (for example by measuring the neutrino energy and momentum) with enough precision to distinguish which one of the different neutrino mass eigenvalues has been detected.

We can derive a general and simple result, bypassing the cumbersome wave-packet analysis, if we restrict our attention to a *stationary* flux of neutrinos. This restriction covers almost all cases of interest mentioned above, but does not hold for a pulsed neutrino beam nor for a short enough supernova neutrino burst (unless experiments only look at enough time-averaged observables). We now show that *a stationary neutrino wave is fully described by its energy spectrum*, and of course by its direction, flavour and maybe spin. This means that a plane wave is the *same thing* as a mixture of short wavepackets, just as the same light can be obtained as a mixture of circular or linear polarizations.

It is convenient to work in the basis of eigenstates of the Hamiltonian. The most generic *pure* state is a superposition of them. In stationary conditions all interferences between states with different energy average to zero,  $\langle e^{i(E-E')t} \rangle = 0$ , when computing any physical observable.

We need to generalize this proof to a neutrino flux described by a density matrix  $\rho$ . In fact, let us consider e.g. a neutrino produced in  $\pi$  decay,  $\pi \rightarrow \nu_\mu\bar{\mu}$ . A wave function describes the neutrino and the muon. As usual, when we want we restrict to a subset (the neutrino) of the full

system (neutrino and muon), we are forced to introduce mixed states. Furthermore, the particle that produces the neutrino usually interacts in a non negligible way with its surroundings (e.g. a stopped  $\pi$  at FermiLab, or a  ${}^7\text{Be}$  in the sun): using a density matrix for neutrinos is simpler than studying the wave function of FermiLab, or of the sun.

For a mixed state, the proof can be obtained with a little more formalism. Since we assumed stationarity,  $\dot{\rho} = 0$ , and since  $i\dot{\rho} = [H, \rho]$ , the ‘off-diagonal’ elements of  $\rho$  between states with different energy vanish. Neutrinos with different mass and the same energy oscillate, as we now describe.

We begin with considering two generation mixing, so that we just have one mixing angle,  $\theta$ , and no CP violation. We assume that at the production region,  $x \approx 0$ ,  $\nu_e$  are produced with energy  $E$ . To study their propagation it is convenient to utilize the basis of neutrino mass eigenstates  $\nu_{1,2}$ , and write  $|\nu(x=0)\rangle = |\nu_e\rangle = \cos\theta|\nu_1\rangle + \sin\theta|\nu_2\rangle$ . Since  $\nu_1$  and  $\nu_2$  have different masses, the initial  $\nu_e$  becomes some other mixture of  $\nu_1$  and  $\nu_2$ , or equivalently of  $\nu_\mu$  and  $\nu_e$ . At a generic  $x$

$$|\nu(x)\rangle = e^{ip_1x} \cos\theta|\nu_1\rangle + e^{ip_2x} \sin\theta|\nu_2\rangle.$$

The probability of  $\nu_\mu$  *appearance* at the detection region  $x \approx L$  is

$$P(\nu_e \rightarrow \nu_\mu) = |\langle\nu_\mu|\nu(L)\rangle|^2 = \sin^2 2\theta \sin^2 \frac{(p_2 - p_1)L}{2} \simeq \sin^2 2\theta \sin^2 \frac{\Delta m_{12}^2 L}{4E}. \quad (4)$$

Since in all cases of experimental interest  $E \gg m_i$ , in the final passage we have used the ultra-relativistic approximation  $p_i = E - m_i^2/2E$ , valid at dominant order in the small neutrino masses and defined  $\Delta m_{12}^2 \equiv m_2^2 - m_1^2$ .<sup>4</sup>

By swapping the names of the two mass eigenstates,  $\nu_1 \leftrightarrow \nu_2$ , one realizes that the couples  $(\theta, \Delta m_{12}^2)$  and  $(\pi/2 - \theta, -\Delta m_{12}^2)$  describe the same physics. On the contrary  $(\theta, \Delta m_{12}^2)$  and  $(\pi/2 - \theta, \Delta m_{12}^2)$  are physically different. However, eq. (4) shows that vacuum oscillations depend only on  $\sin^2 2\theta$  and do not discriminate these two cases. Oscillation effects are maximal at  $\theta = \pi/4$ .

The  $\nu_e$  *disappearance* probability is

$$P(\nu_e \rightarrow \nu_e) = |\langle\nu_e|\nu(L)\rangle|^2 = 1 - P(\nu_e \rightarrow \nu_\mu).$$

Numerically

$$S_{ij} \equiv \sin^2 \frac{\Delta m_{ij}^2 L}{4E} = \sin^2 1.27 \frac{\Delta m_{ij}^2}{\text{eV}^2} \frac{L}{\text{Km}} \frac{\text{GeV}}{E}. \quad (5)$$

The oscillation wave-length is  $\lambda = 4\pi E/\Delta m^2 = 2.48 \text{ km}(E/\text{GeV})(\text{eV}^2/\Delta m_{ij}^2)$ . In order to see oscillations one needs neutrinos of low enough energy, that have small detection cross sections (section 5). Furthermore, one recognizes a  $\nu_\tau$  scattering event by detecting a scattered  $\tau$ . In  $\nu_\tau e \rightarrow \nu_e \tau$  one needs  $E_{\nu_\tau} \gtrsim m_\tau$ .

---

<sup>4</sup>We sketch the standard over-simplified derivation. It proceeds writing the evolution in *time* as  $|\nu(t)\rangle = e^{iHt}|\nu(0)\rangle$ . Assuming that neutrinos with different mass have equal momentum, the hamiltonian is  $H \approx p + mm^\dagger/2p$ . This gives the correct final formula, if one does not take into account that different neutrinos have different velocity. It is not clear which ‘time’ one should use (e.g. when neutrinos are produced by slow decays), as no real experiment measures it: experiments measure the *distance* from the production point.

Furthermore, in many realistic cases neutrinos actually oscillate in space but not in time, because their wave-packets have a much larger spread in momentum than in energy. This happens because the particle that decays into neutrinos often interacts with a *big* environment and therefore behaves like a ball that bounces in a box: keeping the same energy but changing momentum.

All this discussion applies to oscillations, not only to neutrino oscillations.

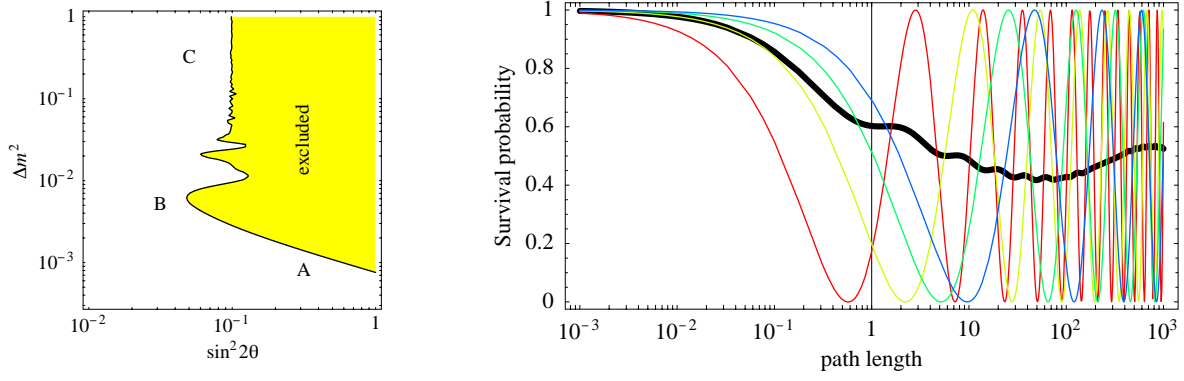


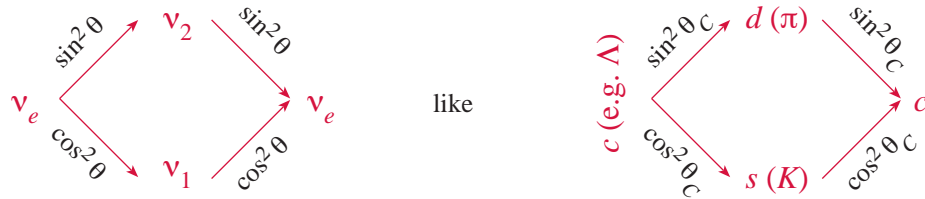
Figure 4: (a) Typical bound on oscillations. (b) Averaging of oscillations of neutrinos with different energy.

In a realistic setup, the neutrino beam is not monochromatic, and the energy resolution of the detector is not perfect: one needs to average the oscillation probability around some energy range  $\Delta E$ . Furthermore, the production and detection regions are not points: one needs to average around some path-length range  $\Delta L$ . Including these effects, in fig. 4a we show a typical experimental bound on oscillations. We can distinguish three regions:

- A **Oscillations with short base-line**, where  $S_{ij} \ll 1$ . In this limit  $P(\nu_e \rightarrow \nu_\mu) \simeq \sin^2 2\theta \cdot (\Delta m^2)^2 \times (L/4E)^2$ . This explains the slope of the exclusion region in part A of fig. 4a. Next, we see that  $P(\nu_e \rightarrow \nu_\mu) \propto L^2$ . Since going far from an approximatively point-like neutrino source the neutrino flux decreases as  $1/L^2$ , fixing the optimal location for the detector is usually not a straightforward choice.
- B **Averaged oscillations**, where  $\langle S_{ij} \rangle = 1/2$  as illustrated in fig. 4b. In this limit one has

$$P(\nu_e \rightarrow \nu_\mu) = \frac{1}{2} \sin^2 2\theta, \quad P(\nu_e \rightarrow \nu_e) = 1 - \frac{1}{2} \sin^2 2\theta. \quad (6)$$

The information on the oscillation phase is lost due to the insufficient experimental resolution in  $E$  or  $L$ . Consequently, one can rederive the transition probabilities (6) by combining *probabilities* rather than *amplitudes*. The computation proceeds in full analogy to the our  $\pi/K$  example at page 11, as illustrated by the following figure:



At  $x \approx 0$  one produces:

- a  $\nu_1$  with probability  $\cos^2 \theta$  (later detected as a  $\nu_\mu$  with probability  $\sin^2 \theta$ , or as a  $\nu_e$  with probability  $\cos^2 \theta$ ), and

- a  $\nu_2$  with probability  $\sin^2 \theta$  (later detected as a  $\nu_\mu$  with probability  $\cos^2 \theta$ , or as a  $\nu_e$  with probability  $\sin^2 \theta$ ).

Therefore one obtains the same result as in (6)

$$P(\nu_e \rightarrow \nu_\mu) = 2 \sin^2 \theta \cos^2 \theta, \quad P(\nu_e \rightarrow \nu_e) = \sin^4 \theta + \cos^4 \theta.$$

We now discuss in more detail how the averaging over the energy spectrum, transforms coherent oscillations into an incoherent process.

**C The intermediate region.** Due to the finite energy resolution  $\Delta E$  of the experimental apparatus, coherence is lost when neutrinos of different energy have too different oscillation phases  $\phi \sim \Delta m^2 L / E$ , i.e. when

$$\Delta \phi \approx \frac{\Delta E}{E} \phi \gtrsim 1 \quad (7)$$

Therefore one can see  $n \sim E / \Delta E$  oscillations before they average out. So far it has not been possible to see even the first oscillation.<sup>5</sup>

## 4.2 Oscillations in vacuum: useful formulæ

Before specializing to the three generation case, we quote some general results

- **Conservation of probability** implies

$$\sum_{\ell'} P(\nu_\ell \rightarrow \nu_{\ell'}) = 1$$

- **CPT-invariance** implies

$$P(\nu_\ell \rightarrow \nu_{\ell'}) = P(\bar{\nu}_{\ell'} \rightarrow \bar{\nu}_\ell)$$

- In many situations **CP-invariance** approximately holds and implies

$$P(\nu_\ell \rightarrow \nu_{\ell'}) = P(\bar{\nu}_\ell \rightarrow \bar{\nu}_{\ell'})$$

Together with CPT-invariance, CP-invariance is equivalent to **T invariance**

$$P(\nu_\ell \rightarrow \nu_{\ell'}) = P(\nu_{\ell'} \rightarrow \nu_\ell)$$

Therefore  $T$  conserving (breaking) contributions are even (odd) in  $L$ .

---

<sup>5</sup>The energy resolution of the experiment usually gives the dominant contribution to the total  $\Delta E$ . Still, one can wonder how and when loss of coherence arises in an ideal set-up. In the wave-packet language, coherence is lost when the wave-packets corresponding to different mass eigenstates (that move at different velocities  $\Delta v \sim \Delta m^2 / E^2$ ) no longer overlap. This happens when

$$\Delta v \cdot t \gtrsim \Delta x \quad (8)$$

where  $\Delta x$  is the size of the wave-packet.

In the stationary case that we are considering, this same effect is accounted by the energy average over the minimal  $\Delta E$  demanded by quantum mechanics, approximatively equal to  $\Delta E \approx 1 / \Delta x$ , as dictated by the uncertainty relation  $\Delta x \cdot \Delta p \gtrsim \hbar$ . In fact, one can verify that eq. (7) and (8) are equivalent. **Poco chiaro**

This effect is hardly relevant. A supernova pulse could be as short as  $\Delta x \sim 0.1$  s. After traveling for cosmological distances

$$\Delta v \cdot t \approx L \frac{\Delta m^2}{E^2} \approx 0.1 \text{ s} \frac{L}{10^{25} \text{ m}} \frac{\Delta m^2}{3 \cdot 10^{-3} \text{ eV}^2} \left( \frac{100 \text{ MeV}}{E} \right)^2$$

For the Be line...



Up to an irrelevant overall phase, the transition amplitude is

$$A(\nu_\ell \rightarrow \nu_{\ell'}) = \langle \nu_{\ell'} | \nu_\ell(L) \rangle = \langle \nu_{\ell'} | U(L) | \nu_\ell \rangle = \sum_i w_i^{\ell\ell'} e^{i\delta_i}, \quad U(L) = \exp\left(i \frac{\mathbf{m}^\dagger \mathbf{m} L}{2E}\right) \quad (9)$$

where

$$w_i^{\ell\ell'} \equiv V_{\ell'i}^* V_{\ell i}, \quad \delta_i \equiv \frac{m_i^2 L}{2E}, \quad \delta_{ij} \equiv \delta_i - \delta_j.$$

We see that Majorana phases do not affect oscillations. In the short base-line limit, approximating  $\exp i\boldsymbol{\delta} \simeq \mathbb{I} + i\boldsymbol{\delta} + \dots$  (here  $\boldsymbol{\delta}$  is a flavour matrix), the oscillation probability reduces to the well known ‘Fermi golden rule’,  $P(\nu_\ell \rightarrow \nu_{\ell'}) = |\delta_{\ell\ell'}|^2$  for  $\ell \neq \ell'$ .

Eq. (9) is used in numerical computations; however when  $\delta_i \gg 1$  the result rapidly oscillates around some mean value, that is cumbersome to compute numerically. In the simple case of vacuum oscillations it is possible and convenient to rewrite eq. (9) in a longer but more useful form. Using  $e^{i\delta} = 1 - 2\sin^2(\delta/2) + i\sin\delta$ , from eq. (9) we get

$$\begin{aligned} P(\nu_\ell \rightarrow \nu_{\ell'}) &= |A(\nu_\ell \rightarrow \nu_{\ell'})|^2 = \sum_{ij} w_i^{\ell\ell'} w_j^{\ell\ell'*} (1 - 2\sin^2 \frac{\delta_{ij}}{2} + i\sin\delta_{ij}) \\ &= \delta_{\ell\ell'} - \sum_{i<j} 4\text{Re } w_i^{\ell\ell'} w_j^{\ell\ell'*} \sin^2 \frac{\delta_{ij}}{2} - \sum_{i<j} 2\text{Im } w_i^{\ell\ell'} w_j^{\ell\ell'*} \sin\delta_{ij}. \end{aligned}$$

The last terms violates CP. Specializing to the case of 3 neutrinos

$$P(\nu_\ell \rightarrow \nu_{\ell'}) = \delta_{\ell\ell'} + p_{\ell\ell'}^{12} S_{12} + p_{\ell\ell'}^{13} S_{13} + p_{\ell\ell'}^{23} S_{23} - 8J \sum_{\ell''} \epsilon_{\ell\ell'\ell''} \sin \frac{\delta_{12}}{2} \sin \frac{\delta_{13}}{2} \sin \frac{\delta_{23}}{2} \quad (10)$$

where

$$p_{ii'}^{\ell\ell'} = -4\text{Re } V_{\ell i} V_{\ell' i'} V_{\ell i}^* V_{\ell' i'}^*, \quad p_{ii'}^{\ell\ell} = -4|V_{\ell i} V_{\ell' i'}|^2.$$

We have rewritten the CP-violating term using

$$\text{Im } V_{\ell i} V_{\ell' i'} V_{\ell i}^* V_{\ell' i'}^* = J \sum_{j'', i''} \epsilon_{ii' i''} \epsilon_{jj' j''} \quad \text{where} \quad J = -\frac{1}{4} \cos\theta_{13} \sin 2\theta_{13} \sin 2\theta_{12} \sin 2\theta_{23} \cdot \sin\phi$$

and

$$\sin\delta_{12} + \sin\delta_{23} + \sin\delta_{31} = 4\sin(\delta_{12}/2)\sin(\delta_{23}/2)\sin(\delta_{13}/2).$$

As expected the CP-violating contribution is odd in  $L$ . In the small  $L$  limit, it is proportional to  $L^3$ . It is small when any mixing angle  $\theta_{ij}$  or any oscillation phase  $\delta_{ij}$  is small; it averages to zero when some  $\delta_{ij} \gg 1$ . These properties explain why it is difficult to observe CP-violation.

The maximal possible value of  $J$  is  $1/6\sqrt{3}$ , obtained for  $\theta_{12} = \theta_{23} = \pi/4$  and  $\cos^2\theta_{13} = 2/3$ . The corresponding formulæ for antineutrinos are obtained by exchanging  $V \leftrightarrow V^*$ , so that in the final formula only the sign of the CP-violating term changes.

Data indicate that

$$|\Delta m_{13}^2| \approx |\Delta m_{23}^2| = \Delta m_{\text{atm}}^2 \approx 3 \cdot 10^{-3} \text{ eV}^2, \quad \Delta m_{12}^2 = \Delta m_{\text{sun}}^2 < 3 \cdot 10^{-4} \text{ eV}^2.$$

Therefore it is interesting to consider the limit  $\Delta m_{23}^2 \gg \Delta m_{12}^2$ , i.e.  $S_{13} \approx S_{23}$  so that we can simplify

$$p_{\ell\ell'}^{13} + p_{\ell\ell'}^{23} = -4\text{Re } w_3^{\ell\ell'} (w_1^{\ell\ell'*} + w_2^{\ell\ell'*}) = -4\text{Re } w_{\ell\ell'}^3 (\delta_{\ell\ell'} - w_3^{\ell\ell'*}).$$



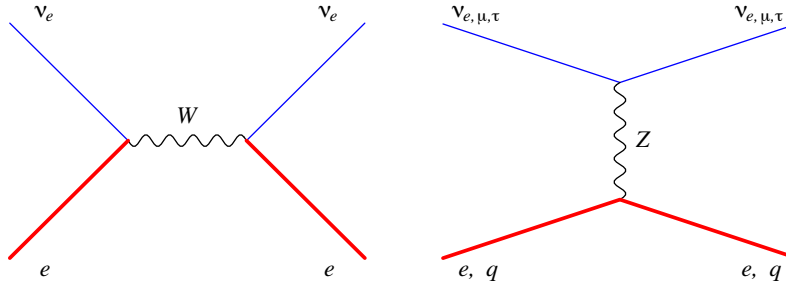


Figure 5: *Interactions of neutrinos with electrons and quarks.*

For simplicity, we now write explicit expressions valid for the CP-conserving case:

$$\begin{aligned} P(\nu_\ell \rightarrow \nu_\ell) &= 1 - 4V_{\ell 1}^2 V_{\ell 2}^2 S_{12} - 4V_{\ell 3}^2 (1 - V_{\ell 3}^2) S_{23} \\ P(\nu_\ell \rightarrow \nu_{\ell'}) &= -4V_{\ell 1} V_{\ell 2} V_{\ell' 1} V_{\ell' 2} S_{12} + 4V_{\ell 3}^2 V_{\ell' 3}^2 S_{23}. \end{aligned}$$

Special interesting sub-cases are:  $S_{12} \approx 0$  (the baseline is so short that solar oscillations cannot be seen)  $S_{23} \approx 1/2$  (the baseline is so long that atmospheric oscillations are averaged).

Finally, in the limit of fully averaged oscillations,  $\langle S_{12} \rangle = \langle S_{23} \rangle = 1/2$ , one can reobtain the survival probability by combining probabilities:

$$P(\nu_\ell \rightarrow \nu_{\ell'}) = \sum_i |V_{\ell i} V_{\ell' i}|^2.$$

### 4.3 Oscillations in matter

The probability that a neutrino of energy  $E \sim \text{MeV}$  get scattered while crossing the earth  $\sim 10^{-12}$  (section 5). Neutrinos of ordinary energies cross the earth or the sun without being significantly absorbed. Still, the presence of matter can significantly affect neutrino propagation. This apparently unusual phenomenon has a well known optical analogue. A transparent medium like air or water negligibly absorbs light, but still significantly reduces its speed:  $v = c/n$ , where  $n$  is the ‘refraction index’. In some materials  $n$  is different for different polarizations of light, giving rise to characteristic effects. The same thing happens for neutrinos. Since matter is composed by electrons (rather than by  $\mu$  and  $\tau$ ),  $\nu_e$  interact differently than  $\nu_{\mu, \tau}$ , giving rise to a flavour-dependent refraction index, that we now compute.

*Forward* scattering of neutrinos interferes with free neutrino propagation, giving rise to refraction. Scattering of  $\nu_\ell$  on electrons and quarks mediated by the  $Z$  boson (fig. 5b) is the same for all flavours  $\ell = \{e, \mu, \tau\}$ , and therefore does not affect flavour transitions between active neutrinos. The interesting effect is due to  $\nu_e e$  scattering mediated by the  $W$  boson (fig. 5a), that is described at low energy by the effective Hamiltonian

$$\mathcal{H}_{\text{eff}} = \frac{4G_F}{\sqrt{2}} (\bar{\nu}_e \gamma_\mu P_L \nu_e) (\bar{e} \gamma_\mu P_L e).$$

In a background composed by non relativistic electrons and no positrons (e.g. the earth, and to a very good approximation the sun) one has

$$\langle \bar{e} \gamma_\mu \frac{1 - \gamma_5}{2} e \rangle = \frac{N_e}{2} (1, 0, 0, 0)_\mu \quad \text{and therefore} \quad \langle \mathcal{H}_{\text{eff}} \rangle = \sqrt{2} G_F N_e (\bar{\nu}_e \gamma_0 P_L \nu_e)$$

medium	$V_{\text{CC}}$ for $\nu_e, \bar{\nu}_e$ only	$V_{\text{NC}}$ for $\nu_{e,\mu,\tau}, \bar{\nu}_{e,\mu,\tau}$
$e, \bar{e}$	$\pm\sqrt{2}G_{\text{F}}(N_e - N_{\bar{e}})$	$\mp\sqrt{2}G_{\text{F}}(N_e - N_{\bar{e}})(1 - 4s_{\text{W}}^2)/2$
$p, \bar{p}$	0	$\pm\sqrt{2}G_{\text{F}}(N_p - N_{\bar{p}})(1 - 4s_{\text{W}}^2)/2$
$n, \bar{n}$	0	$\mp\sqrt{2}G_{\text{F}}(N_n - N_{\bar{n}})/2$
ordinary matter	$\pm\sqrt{2}G_{\text{F}}N_e$	$\mp\sqrt{2}G_{\text{F}}N_n/2$

Table 1: *Matter potentials for  $\nu$  (upper sign) and  $\bar{\nu}$  (lower sign).*

where  $N_e$  is the electron number density. Including also the  $Z$ -contribution<sup>6</sup>, the effective matter Hamiltonian in ordinary matter is

$$\langle \mathcal{H}_{\text{eff}} \rangle = (\bar{\nu}_\ell V \gamma_0 P_L \nu_\ell) \quad \text{where} \quad V = \sqrt{2}G_{\text{F}} \left[ N_e \text{diag}(1, 0, 0) - \frac{N_n}{2} \text{diag}(1, 1, 1) \right] \quad (11)$$

is named ‘matter potential’ and is a flavour matrix. Adding this matter term to the Hamiltonian describing free propagation of an ultra-relativistic neutrino, one obtains a modified relation between energy and momentum (i.e. a ‘refraction index’), as we now discuss.<sup>7</sup>

## 4.4 Majorana vs Dirac neutrinos

It is easy to see that pure Majorana neutrinos oscillate in vacuum in the same way as pure Dirac neutrinos. Looking only at vacuum oscillations it is not possible to experimentally discriminate the two cases. The additional CP-violating phases present in the Majorana case do not affect oscillations.

It is less easy to realize that, in the realistic case of ultrarelativistic neutrinos, this unpleasant result continues to hold also for oscillations in matter:

<sup>6</sup>One needs to evaluate quark currents  $\bar{q}\gamma_\mu q$  over a background of normal matter. The result is shown in table 1. Non obvious but well known properties of the quark currents guarantee that the naïve result, written in terms of proton and neutron number densities  $N_n$  and  $N_p$  by simply using  $p = uud$  and  $n = udd$ , is correct. ‘Ordinary matter’ is composed by electrons, protons, neutrons with  $N_p = N_e$  (no net electric charge) and  $N_n \approx N_p$ . The mass density is  $\rho \approx m_p N_p + m_n N_n$ . At tree level matter effects do not distinguish  $\nu_\mu$  from  $\nu_\tau$ ; loop effects generate a small difference of order  $(m_\tau/M_W)^2 \sim 10^{-5}$  [2].

<sup>7</sup>A note about neutrino oscillations in the early universe. At temperatures  $T \gg m_e$  one has large densities of electrons and positrons, but they are almost equal:  $N_e = N_{\bar{e}} \sim T^3$ . Therefore matter effects, proportional to  $N_e - N_{\bar{e}}$ , almost cancel out. The subleading term in the low-energy expansion of the  $W, Z$  propagators  $(1/(k^2 - M^2)) \approx -1/M^2 - k^2/M^4 + \dots$  for  $k \ll M$  induces a potentially dominant contribution to the matter potential  $V$ , of order  $G_{\text{F}}^2 E_\nu (E_e N_e + E_{\bar{e}} N_{\bar{e}}) \sim G_{\text{F}}^2 T^5$ .

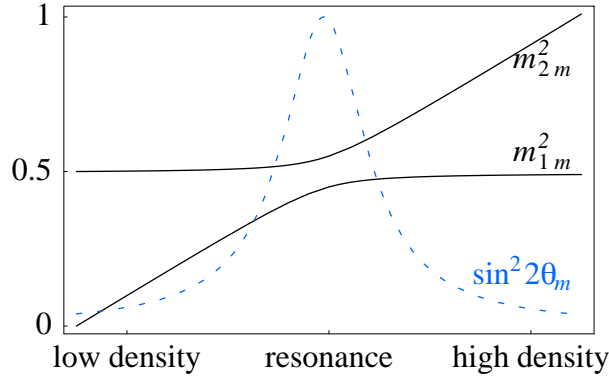


Figure 6: *Effective masses and mixing angle in matter for two neutrino flavours as a function of the density. We take  $\theta = 0.1$ ,  $\Delta m^2 = 1/2$  (arbitrary units).*

**Majorana** Only left-handed neutrinos exist. Their equation of motion is

$$(i\partial - V\gamma_0)\nu_L = m\nu_L$$

where  $m$  is a Majorana mass term. Squaring, one obtains the dispersion relation

$$(E - V)^2 - p^2 = m^2$$

that in the ultrarelativistic limit becomes

$$p \simeq E - \left(\frac{mm^\dagger}{2E} + V\right).$$

**Ho messo  $mm^\dagger$  a caso, come salta fuori?**

**Dirac** Neutrinos have both a left and a right-handed component. Their equation of motion is

$$\begin{cases} i\partial\nu_L = m\nu_R + V\gamma_0\nu_L \\ i\partial\nu_R = m\nu_L \end{cases}$$

where  $m$  is a Dirac mass term. Eliminating  $\nu_R$  and assuming that  $V$  is constant one gets

$$[\partial^2 + m^2 + V i\partial\gamma_0]\nu_L = 0.$$

In the ultrarelativistic limit  $i\partial\gamma_0\nu_L \simeq 2i\partial_0\nu_L$ , giving the dispersion relation

$$p \simeq E - \left(\frac{mm^\dagger}{2E} + V\right).$$

The density of ordinary matter negligibly changes on a length scale  $\sim 1/E$ , so that the gradient of  $V$  can indeed be neglected.

*In conclusion, oscillations in matter of ultrarelativistic neutrinos are described by the equation*

$$i\frac{d}{dx}\nu = H\nu, \quad \text{where} \quad H = \frac{m^\dagger m}{2E} + V, \quad \nu = \begin{pmatrix} \nu_e \\ \nu_\mu \\ \nu_\tau \end{pmatrix}, \quad (12)$$

*that can be solved starting from the production point knowing which flavour is there produced.  $V$  is given in eq. (11). For anti-neutrinos one needs to change  $V \rightarrow -V$  (ordinary matter is not CP-invariant).*

The matter density can depend on both time and position, but usually it depends only on the position (e.g. in the sun). Sometimes it is roughly constant (e.g. in the earth mantle), and it is convenient to define effective energy-dependent neutrino mass eigenvalues  $m_m^2$ , eigenvectors  $\nu_m$

and mixing angles  $\theta_m$  in matter by diagonalizing  $m^\dagger m + 2EV$ . In the simple case with only the  $\nu_e$  and  $\nu_\mu$  flavours, the oscillation parameters in matter are

$$\tan 2\theta_m = \frac{A}{B}, \quad \Delta m_m^2 = \sqrt{A^2 + B^2}, \quad \text{where} \quad \begin{aligned} A &\equiv \Delta m^2 \sin 2\theta, \\ B &\equiv \Delta m^2 \cos 2\theta \mp 2\sqrt{2}G_F N_e E \end{aligned} \quad (13)$$

and  $\theta$  and  $\Delta m^2$  are the oscillation parameters in vacuum. The  $- (+)$  sign holds for  $\nu$  ( $\bar{\nu}$ ).

Fig. 6 shows a numerical example. The most noticeable features are:

- Unlike vacuum oscillations, **matter oscillations distinguish  $\theta$  from  $\pi/2 - \theta$** . Consequently  $\sin^2 2\theta$  (used in fig. 4a) is no longer a good variable; it is customary to use  $\tan^2 \theta$ . Not caring of the sign of  $\theta_m - \pi/4$ , eq. (13) can be rewritten as

$$\sin^2 2\theta_m = \frac{\sin^2 2\theta}{\lambda^2}, \quad \Delta m_m^2 = \lambda \cdot \Delta m^2, \quad \lambda = \sqrt{\sin^2 2\theta + \left( \cos^2 2\theta \mp \frac{2\sqrt{2}G_F N_e E}{\Delta m^2} \right)^2}.$$

- **Resonance.** If  $\Delta m^2 \cos 2\theta > 0$  ( $< 0$ ) the matter contribution can render equal the diagonal elements of the effective neutrino (anti-neutrino) mass matrix, so that  $\theta_m$  can be maximal,  $\theta_m = \pi/4$ , even if  $\theta \ll 1$ . At the resonance  $\Delta m_m^2 = \Delta m^2 \sin 2\theta$ . Matter effects resonate at

$$E \sim \frac{\Delta m^2}{2\sqrt{2}G_F N_e} = 3 \text{ GeV} \frac{\Delta m^2}{10^{-3} \text{ eV}^2} \frac{1.5 \text{ g/cm}^3}{\rho Y_e}. \quad (14)$$

The typical electron number density of ordinary matter is  $N_e \sim 1/\text{\AA}^3$ . For example, the density of the mantle of the earth is  $\rho \approx 3 \text{ g/cm}^3$  and therefore  $N_e = \rho Y_e / m_n = 1.5 N_A / \text{cm}^3$ , where  $N_A = 6.022 \cdot 10^{23}$  is the Avogadro number and  $Y_e \equiv N_e / (N_n + N_p) \approx 0.5$ . Other characteristic densities are  $\rho \sim 10 \text{ g/cm}^3$  in the earth core,  $\rho \sim 100 \text{ g/cm}^3$  in the solar core, and  $\rho \sim m_n^4 \sim 10^{14} \text{ g/cm}^3$  in a supernova. The density profiles of the earth and of the sun are plotted in fig. 7.

- **Matter-dominated oscillations.** When neutrinos have high enough energy the matter term dominates: being flavour-diagonal it suppresses oscillations. In this situation, neutrinos oscillate in matter with an energy-independent wave-length  $\lambda = \pi / \sqrt{2} G_F N_e$ . In the earth mantle  $\lambda \sim 3000 \text{ km}$ , comparable to the size of the earth.

## 4.5 Oscillations in a varying density

In order to study solar and supernova neutrinos it useful to develop an approximation for the oscillation probabilities for neutrinos produced in the core of the star (where matter effects are important), that escape into the vacuum (where matter effects are negligible). At some intermediate point matter effects can be resonant.

Here, we discuss the case of two neutrino generations in the sun; later it will be easy to generalize the discussion. Briefly, solar neutrinos behave as follows.

1.  $\nu_e$  are produced in the core of the sun,  $r \approx 0$ . The probability of  $\nu_e$  being  $\nu_{1m}$  or  $\nu_{2m}$  are  $\cos^2 \theta_m$  and  $\sin^2 \theta_m$  respectively. When matter effects are dominant  $\nu_e \simeq \nu_{2m}$  (i.e.  $\sin^2 \theta_m = 1$ ).

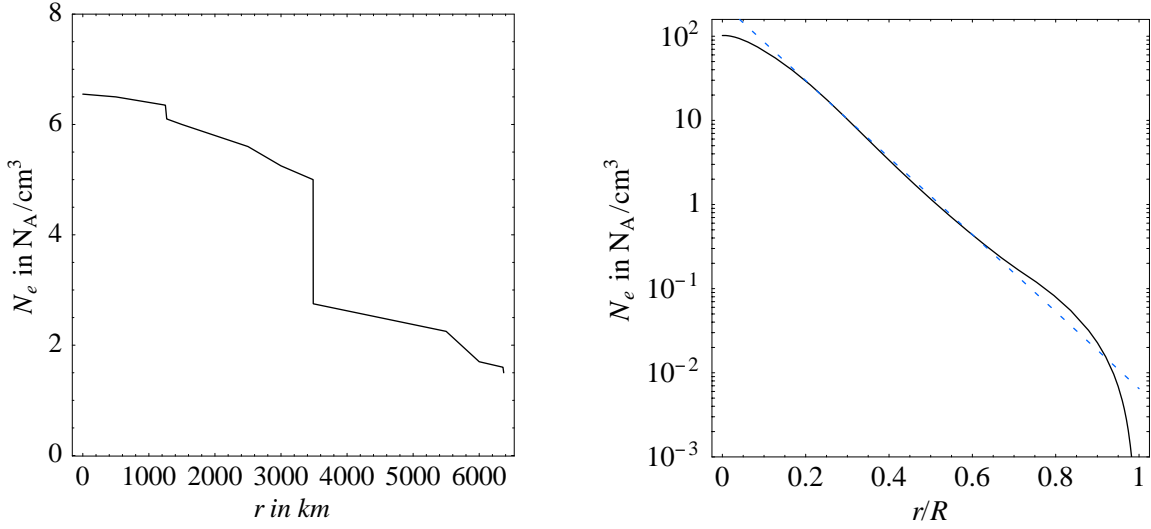


Figure 7: *Density profile of (a) the earth (b) the sun.*

2. The oscillation wave-length  $\lambda$  is much smaller than the solar radius  $R$ . Therefore neutrinos propagate for many oscillation wave-lengths: the phase averages out so that we have to combine probabilities instead of amplitudes. If the density changes very slowly ('adiabatic approximation', see below) each neutrino mass eigenstate will remain the same. Otherwise neutrinos will flip to the other mass eigenstate with some level-crossing probability  $P_C$  that we will later compute:

$$\nu_{2m}(r \approx 0) \text{ evolves to } \begin{cases} \nu_{2m}(r \approx R) = \nu_2 \text{ with probability } 1 - P_C \\ \nu_{1m}(r \approx R) = \nu_1 \text{ with probability } P_C \end{cases}$$

(and similarly for  $1 \leftrightarrow 2$ ).

3. Neutrinos propagate from the sun to the earth, and eventually inside the earth before reaching the detector. For a typical solar neutrino energy,  $E \sim \text{MeV}$ , the first effect is relevant for  $\Delta m^2 \sim 10^{-10} \text{ eV}^2$  (so that the oscillation wave-length is comparable to the earth-sun distance), and the second effect for  $\Delta m^2 \sim 10^{-6} \text{ eV}^2$  (so that earth matter effects are resonant, see eq. (14)). For simplicity we start ignoring these effects.
4. Finally, the  $\nu_1$  ( $\nu_2$ ) is detected as  $\nu_e$  with probability  $\cos^2 \theta$  ( $\sin^2 \theta$ ).

Combining all these probabilities, as summarized in fig. 8, one gets

$$P(\nu_e \rightarrow \nu_e) = \frac{1}{2} + \left(\frac{1}{2} - P_C\right) \cos 2\theta \cos 2\theta_m \quad (15)$$

where  $\theta_m$  is the effective mixing angle at the production point. It is instructive to specialize eq. (15) to three limiting cases:

- a.  $P(\nu_e \rightarrow \nu_e) = P_C$  when  $\cos 2\theta_{2m} = -1$  (i.e. matter effects dominate so that the heavier effective neutrino mass eigenstate is  $\nu_{2m}(0) \simeq \nu_e$ ) and  $\theta \ll 1$ .
- b.  $P(\nu_e \rightarrow \nu_e) = \sin^2 \theta$  when  $\cos 2\theta_{2m} = -1$  and neutrinos propagate adiabatically ( $P_C = 0$ ).

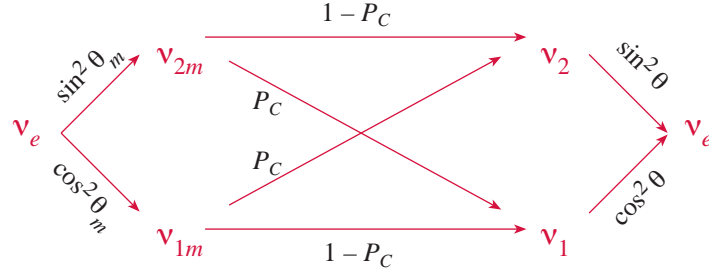


Figure 8: *Propagation of a neutrino from the sun to the earth.*

- c.  $P(\nu_e \rightarrow \nu_e) = 1 - \frac{1}{2} \sin^2 2\theta$  (equal to averaged vacuum oscillations) when  $\cos 2\theta_{2m} = -1$  and in the extreme non-adiabatic limit ( $P_C = \cos^2 \theta$ ). This value of  $P_C$  can be computed by considering very dense matter that abruptly terminates in vacuum. The produced neutrino  $\nu_e \simeq \nu_{2m}$  does not change flavour at the transition region, since it is negligibly short. Therefore  $P_C = |\langle \nu_e | \nu_1 \rangle|^2 = \cos^2 \theta$ .

We now compute  $P_C$  (point 2). We rewrite the evolution equation  $i d\nu/dx = H(x)\nu$  in the new basis of instantaneous matter mass eigenstates  $\nu_m$ , related to the flavour basis by

$$\nu = V_m(x)\nu_m, \quad V_m = \begin{pmatrix} \cos \theta_m & -\sin \theta_m \\ \sin \theta_m & \cos \theta_m \end{pmatrix}.$$

In this new basis the effective Hamiltonian is diagonal,  $H_m = V_m^{-1} H V_m = \text{diag}(m_{1m}^2, m_{2m}^2)/2E$ . However the wave equation contains an additional term due to the fact that the new basis is position-dependent:

$$i \frac{d\nu_m}{dx} = \left( H_m - i V_m^{-1} \frac{dV_m}{dx} \right) \nu_m = \begin{pmatrix} m_{1m}^2/2E & -i d\theta_m/dx \\ i d\theta_m/dx & m_{2m}^2/2E \end{pmatrix} \nu_m. \quad (16)$$

We see that in the extreme adiabatic limit where the density gradient is small enough that we can neglect  $d\theta_m/dx$ , the level-crossing probability is  $P_C = 0$ . The ratio between the difference in the diagonal elements and the off-diagonal element of (16) controls how much adiabaticity is violated. Eq. (13) shows that this ratio is maximal at the resonance point<sup>8</sup>, where it equals

$$\frac{\Delta m_m^2/2E}{d\theta_m/dx} = \gamma \cdot \frac{\sin^2 2\theta}{2\pi \cos 2\theta}, \quad \gamma = \frac{\pi \Delta m^2}{E |d \ln N_e / dr|_{\text{res}}} \approx \frac{\Delta m^2 / E_\nu}{10^{-9} \text{ eV}^2 / \text{MeV}}.$$

The gradient is evaluated around the resonance point, where the density is  $N_e(r) \approx \Delta m^2 / G_F E_\nu$ . In the numerical expression we have approximated the density of the sun as  $N_e = 245 N_A / \text{cm}^3 \times \exp(-10.54 r/R)$  (dashed line in fig. 7b).

In the quasi-adiabatic limit ( $\gamma \gg 1$ ) it would be possible to extract some information on  $P_C$  from elegant considerations. In order to obtain a more accurate and general approximation, it is convenient to proceed in a different way. Around the narrow resonance region one can accurately approximate the complicated solar density profile (fig. 7) with a simple function, such that the wave equation (16) can be solved analytically. Approximating  $N_e$  with an exponential and solving (16) by brute force, one obtains (see [3])

$$P_C = \frac{e^{\gamma \cos^2 \theta} - 1}{e^\gamma - 1}. \quad (17)$$

<sup>8</sup>When  $\Delta m^2 < 0$  does not exist...

When  $\gamma \gg 1$  we go back to the adiabatic approximation,  $P_C = 0$ . In the non-adiabatic limit,  $\gamma \ll 1$ , one gets  $P_C = \cos^2 \theta$  as expected.

The value of  $P_C$  has to be modified in an obvious way if at the production point the sun is not dense enough for giving a resonance. Typically this happens for neutrinos produced somewhat outside the solar core. If in the subsequent propagation the neutrino never enters into the denser region where matter effects are above resonance, one needs to replace  $P_C \rightarrow 0$ . If instead the neutrino crosses this denser region, because produced in the side of the sun far from the earth, one needs to replace  $P_C \rightarrow 2P_C(1 - P_C)$ . This can be easily seen by adding the extra resonance crossing to fig. 8.

## 5 Detecting neutrinos

Neutrinos have only weak interactions: at ordinary energies they cross the earth without being absorbed. Neutrinos can be detected if one has a intense enough flux of neutrinos and a big enough detector with low enough background (that is often placed underground in order to suppress the cosmic-ray background). We now discuss what ‘enough’ means in practice.

### 5.1 Neutrino/electron scattering

According to the SM, the amplitude for scattering of neutrinos on electrons is  $\mathcal{M} \sim G_F m_e E_\nu$ . The total cross section is  $\sigma \sim |\mathcal{M}|^2/s$ , where  $s = (P_e + P_\nu)^2$ . Electrons in atoms have a small velocity  $v \sim \alpha_{\text{e.m.}}$  and can be considered at rest. If  $E_\nu \ll m_e$  one has  $s \sim m_e^2$  and so  $\sigma \sim G_F^2 E_\nu^2$ . If  $E_\nu \gg m_e$  one has  $s \sim m_e E_\nu$  and so  $\sigma \sim G_F^2 m_e E_\nu$ . In the energy range  $m_e \ll E_\nu \ll M_Z^2/m_e$ , the SM prediction at tree level is

$$\sigma(\nu_\ell e) = \frac{2m_e E_\nu G_F^2}{\pi} (G_{L\ell}^2 + \frac{1}{3} G_{R\ell}^2), \quad \sigma(\bar{\nu}_\ell e) = \frac{2m_e E_\nu G_F^2}{\pi} (G_{R\ell}^2 + \frac{1}{3} G_{L\ell}^2). \quad (18)$$

Only  $Z$ -exchange contributes to  $\nu_{\mu,\tau}$  and  $\bar{\nu}_{\mu,\tau}$  scattering on electrons (see fig. 5b). Therefore when  $\ell = \{\mu, \tau\}$  the effective  $G_{L,R\ell}$  are equal to the  $\bar{\ell} Z \ell$  couplings, named  $g_{L,R\ell}$  and listed in table 2 in terms of the weak mixing angle  $s_W^2 \approx 0.223$ . On the contrary  $W$  boson exchange contributes only to  $\nu_e$  and  $\bar{\nu}_e$  scattering on left-handed electrons (see fig. 5a): therefore  $G_{Le} = +\frac{1}{2} + s_W^2 \neq g_{Le}$  and  $G_{Re} = g_{Re}$ , giving rise to a larger cross section. Putting numbers

$$\sigma(\nu_e e) = 0.93\sigma_0, \quad \sigma(\nu_{\mu,\tau} e) = 0.16\sigma_0, \quad \sigma(\bar{\nu}_e e) = 0.39\sigma_0, \quad \sigma(\bar{\nu}_{\mu,\tau} e) = 0.13\sigma_0 \quad (19)$$

where  $\sigma_0 = 10^{-44} \text{cm}^2 E_\nu / \text{MeV}$  and  $E_\nu \gg m_e$ .

SK detects solar neutrinos through  $\nu e$  scattering. With  $10^{10}$  moles of electrons (20.000 ton of water), a flux of  $\text{few} \times 10^6 \nu_e / \text{cm}^2 \text{s}$  with  $E_\nu \sim 10 \text{ MeV}$  (the solar Boron neutrinos), and a 50% efficiency SK can detect about 10000  $\nu_e / \text{yr}$  (finding that about half of them oscillate away). SK and SNO can measure  $T_e = E_e - m_e$ , the kinetic energy of the recoiling electron. Its kinematically allowed range is  $0 \leq T_e \leq E_\nu / (1 + m_e / 2E_\nu)$ . SK and SNO can only detect electrons with  $T_e \gtrsim 5 \text{ MeV}$ . The SM at tree level predicts the energy spectrum of recoil electrons as

$$\frac{d\sigma}{dT_e}(\nu_\ell e \rightarrow \nu_\ell e) = \frac{2G_F^2 m_e}{\pi} [G_{L\ell}^2 + G_{R\ell}^2 (1 - y)^2 - G_{L\ell} G_{R\ell} \frac{m_e}{E_\nu} y] \quad \text{where} \quad y \equiv \frac{T_e}{E_\nu}. \quad (20)$$

The measurement of  $T_e$  alone does not allow to reconstruct  $E_\nu$ , nor allows to discriminate  $\nu_e$  from  $\nu_{\mu,\tau}$ . In principle,  $E_\nu$  can be reconstructed by measuring  $T_e$  and the opening angle  $\vartheta_{\nu e}$  between the



SM fermion	U(1) <sub>Y</sub>	SU(2) <sub>L</sub>	SU(3) <sub>c</sub>	Z couplings	$g_L$	$g_R$
$U = u_R$	$-\frac{2}{3}$	1	$\bar{3}$	$\nu_e, \nu_\mu, \nu_\tau$	$\frac{1}{2}$	0
$D = d_R$	$\frac{1}{3}$	1	$\bar{3}$	$e, \mu, \tau$	$-\frac{1}{2} + s_W^2$	$s_W^2$
$E = e_R$	1	1	1	$u, c, t$	$\frac{1}{2} - \frac{2}{3}s_W^2$	$-\frac{2}{3}s_W^2$
$L = (\nu_L, e_L)$	$-\frac{1}{2}$	2	1	$d, s, b$	$-\frac{1}{2} + \frac{1}{3}s_W^2$	$\frac{1}{3}s_W^2$
$Q = (u_L, d_L)$	$\frac{1}{6}$	2	3			

Table 2: *The SM fermions and their Z couplings.*

incident neutrino and the scattered lepton. However, this angle is small,  $\vartheta_{\nu e} \sim (m_e/E_\nu)^{1/2}$ . When the position of the neutrino source is known (e.g. the sun) measuring  $\vartheta_{\nu e}$  helps in discriminating the signal from the background; when it not known (e.g. a supernova) measuring the direction of the scattered  $e$  helps in locating the source.

## 5.2 Neutrino/nucleon scattering

Similarly, the SM amplitude for scattering of neutrinos on nucleons (i.e. protons or neutrons) is  $\mathcal{M} \sim G_F m_p E_\nu$ . Therefore the total cross section is  $\sigma \sim G_F^2 E_\nu^2$  for  $E_\nu \ll m_p$  and  $\sigma \sim G_F^2 m_p E_\nu$  for  $E_\nu \gg m_p$ . In this case neutrino scattering breaks the nucleon (giving pions and nucleons in the final state) and the cross section is obtained by summing the contributions of the individual neutrino/quark sub-processes. Since  $m_p \gg m_e$  neutrino/nucleon has a larger cross-section than neutrino/electron scattering.

At  $E_\nu \ll m_p$  (e.g. solar and reactor neutrinos), if one is interested only in CC processes (so that the neutrino is converted into a charged lepton, that can be detected) only the reactions  $\bar{\nu}_e p \rightarrow e^+ n$  and  $\nu_e n \rightarrow e p$  are possible ( $\nu_e p \rightarrow e^\pm n$  violates either charge or lepton-number), and only the first one is of experimental interest, because it is not possible to build a target containing enough free neutrons. Enough free protons are obtained using targets made of water (H<sub>2</sub>O), hydrocarbonic scintillators (XXX), etc.

The precise SM prediction is

$$\sigma(\bar{\nu}_e p \rightarrow e^+ n) = \frac{G_F^2 \cos^2 \theta_C}{\pi} (1 + 3a^2) E_e p_e \approx 0.0952 \cdot 10^{-42} \text{ cm}^2 \frac{E_e p_e}{\text{MeV}^2}$$

where  $a = 1.26$  is the axial coupling of nucleon. Beyond having a large cross section, this reaction also allows to reconstruct the neutrino energy. When  $E_\nu \ll m_p$  conservation of energy approximately means  $E_\nu = E_e + m_n - m_p = E_e + 1.293 \text{ MeV}$ . Therefore *the neutrino energy can be deduced* by measuring  $E_e$  alone. Since  $E_e \geq m_e$  this reaction is only possible if  $E_\nu \geq m_e + m_n - m_p = 1.8 \text{ MeV}$ . An analogous expression holds for  $\bar{\nu}_\mu p \rightarrow \mu^+ n$  scattering, that of course has a higher threshold in  $E_\nu$ .

At  $E_\nu \gg m_p$  (e.g. atmospheric and accelerator neutrinos of higher energy) the dominant effect is neutrino/quark scattering. The fact that quarks are bound into a nucleon has no effect on the total ('inclusive') cross-section: the quark  $q^*$  that collides with neutrinos acquires sufficient energy that always finds some way of escaping. Typically  $q^*$  hadronizes picking a  $q\bar{q}$  pair from the vacuum, breaking the nucleon as  $N = qq^* \rightarrow [qqq][\bar{q}q^*] = N\pi$ , giving rise to processes like  $\nu p \rightarrow \ell^+ n \pi^0$  or  $\nu p \rightarrow \ell^+ p \pi^-$ .

One has to sum over all quark sub-processes, taking into account the distribution of quarks in the nucleon (structure functions). Neutrino/quark scattering is similar to electron/quark, and

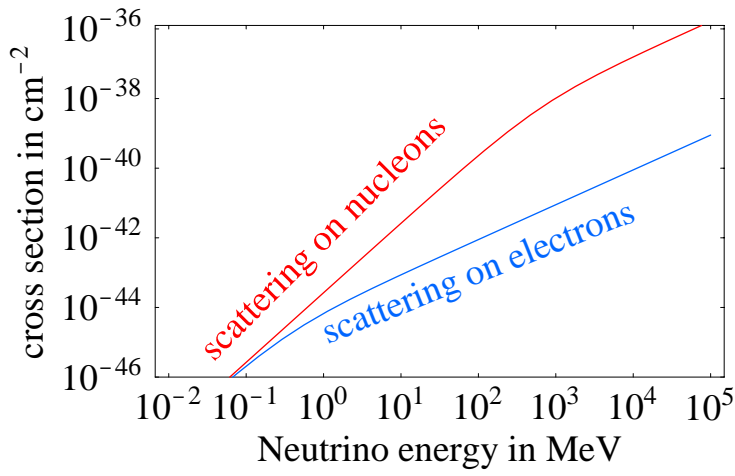


Figure 9: (*per ora*) characteristic neutrino cross sections.

gives a cross section  $\propto G_F E_\nu m_N$ . The  $\nu_\ell$ -quark effective Lagrangian predicted by the SM at tree level is

$$\mathcal{L}_{\text{eff}} = -2\sqrt{2}G_F([\bar{\nu}_\ell\gamma_\alpha\ell_L][\bar{d}_L\gamma^\alpha u_L] + \text{h.c.}) - 2\sqrt{2}G_F \sum_{A,q} g_{Aq}[\bar{\nu}_\ell\gamma_\alpha\nu_\ell][\bar{q}_A\gamma^\alpha q_A]$$

where  $A = \{L, R\}$ ,  $\ell = \{e, \mu, \tau\}$ ,  $q = \{u, d, s, \dots\}$  and the  $Z$  couplings  $g_{Aq}$  are given in table 2 in terms of the weak mixing angle  $s_W \equiv \sin\theta_W$ . The total cross sections for the relevant CC processes are

$$\frac{d\hat{\sigma}}{dy}(\bar{\nu}_\ell\bar{q} \rightarrow \bar{\ell}\bar{q}') = \frac{d\hat{\sigma}}{dy}(\nu_\ell q \rightarrow \ell q') = \frac{G_F^2 \hat{s}}{\pi} R, \quad \frac{d\hat{\sigma}}{dy}(\bar{\nu}_\ell q \rightarrow \bar{\ell}q') = \frac{d\hat{\sigma}}{dy}(\nu_\ell\bar{q} \rightarrow \ell\bar{q}') = \frac{G_F^2 \hat{s}}{\pi} (1-y)^2 R$$

where  $R \equiv (1 + Q^2/M_W^2)^{-1} \approx 1$  in most cases.  $\nu_\ell$  scatters only on  $d$  and  $\bar{u}$  quarks, while  $\bar{\nu}_\ell$  only on  $u$  and  $\bar{d}$  quarks. Consequently  $\nu_\ell$  interacts more strongly with neutrons  $\approx ddu$ , while  $\bar{\nu}_\ell$  with protons  $\approx uud$ . Furthermore  $\nu$  interacts more with  $q$  than with  $\bar{q}$  (the opposite for  $\bar{\nu}$ ). This is due to the factor  $(1-y)^2$  which reduces by 1/3 the integrated cross section.

L'impulso di un partone è  $k = xP$  (dove  $P$  è l'impulso del protone), per cui  $\hat{s} = sx$  e l'integrale sulla distribuzione dei partoni è (ad energie  $E_\nu$  tali che  $R \approx 1$ ) quello che dà la percentuale di impulso del protone portata dal partone:  $p_q = \int_0^1 dx x q(x)$ . Nel protone è

$$p_u + p_c \approx 21\%, \quad p_{\bar{u}} + p_{\bar{c}} \approx 5\%, \quad p_d + p_s + p_b \approx 14.4\%, \quad p_{\bar{d}} + p_{\bar{s}} + p_{\bar{b}} \approx 8\%$$

( $p$  e  $n$  contengono anche una certa quantità di quark-antiquark; la parte di impulso mancante è portata dai gluoni). Il neutrone è più o meno simile con quark di tipo up e down scambiati. So

$$\sigma(\nu_\ell p \rightarrow \ell X) \approx \frac{G_F^2 s}{\pi} (0.14 + \frac{1}{3} 0.05), \quad \sigma(\bar{\nu}_\ell p \rightarrow \bar{\ell} X) \approx \frac{G_F^2 s}{\pi} (\frac{1}{3} 0.21 + 0.08)$$

$$\sigma(\nu_\ell n \rightarrow \ell X) \approx \frac{G_F^2 s}{\pi} (0.21 + \frac{1}{3} 0.08), \quad \sigma(\bar{\nu}_\ell n \rightarrow \bar{\ell} X) \approx \frac{G_F^2 s}{\pi} (\frac{1}{3} 0.14 + 0.05)$$

Un tipico nucleo  $\mathcal{N}$  ha circa  $Z$  protoni e  $Z$  neutroni. Quindi

$$\sigma(\nu\mathcal{N} \rightarrow \ell X) \approx 0.4 Z \frac{G_F^2 s}{\pi} \approx \frac{2ZE_\nu}{\text{GeV}} \times 0.6 \cdot 10^{-38} \text{ cm}^2, \quad \sigma(\bar{\nu}\mathcal{N} \rightarrow \bar{\ell} X) \approx 0.35 Z \frac{G_F^2 s}{\pi}$$

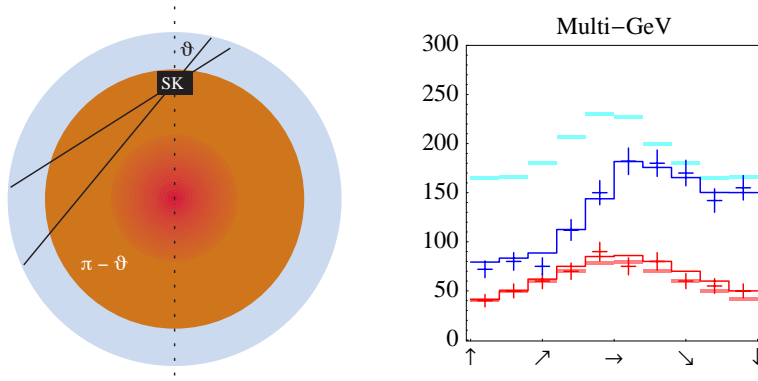


Figure 10: *Since the earth is spheric, without oscillations the flux of atmospheric neutrinos would be up/down symmetric.*

### 5.3 Neutrino/nucleus scattering

## 6 The atmospheric evidence

### 6.1 Atmospheric neutrinos

Atmospheric neutrinos are generated by primary cosmic rays, composed by: 80% protons, 4% He nucleus (i.e. 15% of the total mass), few heavier nuclei. The process can be schematized in 3 steps:

1. Primary cosmic rays hit the nuclei of air in the upper part of the atmosphere, producing mostly pions (and some kaon).
2. Charged pions fastly decay generating muons and muonic neutrinos:

$$\pi^+ \rightarrow \mu^+ \nu_\mu, \quad \pi^- \rightarrow \mu^- \bar{\nu}_\mu$$

(the decay rate into electrons is suppressed by  $m_e^2/m_\mu^2$ ). The total flux of  $\nu_\mu, \bar{\nu}_\mu$  neutrinos is about  $0.1/\text{cm}^2\text{s}$  at  $E_\nu \sim \text{GeV}$  with an error of few 10% (mostly due to the uncertainty in the flux of cosmic rays). At higher energy the flux  $d\Phi/d\ln E_\nu$  approximately decreases as  $E_\nu^{-2}$ . The few kaons decay like pions, except that  $K \rightarrow \pi e^+ \nu_e$  decays are not entirely negligible.

3. The  $\mu$  produced in  $\pi$ -decay travel for a distance

$$L \approx \tau_\mu \frac{E_\mu}{m_\mu} \approx \text{km} \frac{E_\mu}{0.3 \text{ GeV}} \text{check}$$

where  $\tau_\mu$  is the muon life-time and  $E_\mu/m_\mu$  is the relativistic dilatation factor. If all muons can decay,  $\mu \rightarrow e \nu_\mu \bar{\nu}_e$ , one gets a flux of  $\nu_\mu$  and  $\nu_e$  in proportion 2 : 1, with comparable energy, larger than  $\sim 100 \text{ MeV}$ . Muons with energy above few GeV can collide with the earth before decaying, so that at higher energy one has less  $\nu_e$ : the  $\nu_\mu : \nu_e$  ratio is larger than 2.

## 6.2 SuperKamiokande

SK detects neutrinos of energy  $\gtrsim 100$  MeV through CC scattering on nucleons,  $\nu_\ell N \rightarrow \ell N$ . SK is composed by 50000 ton of water (an olympic pool) surrounded by photomultipliers. A relativistic charged lepton  $\ell$  traveling in water give rise to a Cerenkov ring. SK can distinguish  $\nu_\mu$  from  $\nu_e$  (because a scattered  $\mu$  or  $\bar{\mu}$  produces a clean Cerenkov ring, while an  $e$  or  $\bar{e}$  a fuzzy ring), but cannot distinguish  $\nu$  from  $\bar{\nu}$ . Furthermore SK measures the energy  $E_\ell$  and the direction  $\vartheta_\ell$  of the scattered charged lepton. This is not sufficient to reconstruct the neutrino energy,  $E_\nu \gtrsim E_\ell$ . When SK receives a neutrino beam from a known source (KEK in the K2K experiment), it is possible to reconstruct the neutrino energy from  $E_\ell$  and  $\vartheta_{\ell\nu}$  (the opening angle between the incoming neutrino and the scattered lepton):

$$E_\nu = \frac{m_N E_\ell - m_\ell^2/2}{m_N - E_\ell + p_\ell \cos \vartheta_{\ell\nu}} ??$$

However, atmospheric neutrinos arrive from all directions. In practice one has few big energy ‘bins’ from events

1. sub-GeV events, defined as those with  $E_\ell < XX$ . The mean opening angle between the incoming neutrino and the detected charged lepton is about  $\vartheta_{\ell\nu} \sim 60^\circ$ : this sample has a poor angular resolution.
2. multi-GeV. The mean opening angle between the incoming neutrino and the detected charged lepton is about XXX (better at higher energy).
3. passing. So energetic that exit from SK
4. through-going up  $\mu$ : These events are generated by  $\nu_\mu$  that crossed the earth and interacted with the rock below SK, that observes...

A particularly useful quantity are the *energy spectra of parent neutrinos* in absence of oscillations. They can be computed in terms of the more-or-less known neutrino fluxes, cross sections, detector efficiencies, and the result is shown in fig. ???. This is a useful quantities, because the observed can be written as

$$\int dE_\nu P_{\mu\mu}(E_\nu)$$

Fig. ??? shows that atmospheric neutrinos cover a *wide energy range*, from less than a GeV to more than a TeV. Atmospheric neutrinos also allow to probe a *wide range of baselines*, between 10 and 10000 km. Down-ward going neutrinos travel  $h \sim 10$  km ( $h$  is the height of the earth atmosphere); up-ward neutrinos travel  $D_E$  ( $D_E = 12750$  km is the earth diameter).

The crucial point is that in absence of oscillations, according to Gauss theorem, the neutrino rate would be up/down symmetric, i.e. it would not distinguish  $\pm \cos \vartheta$ . (would be flat, horizontal neutrinos cross more atmosphere than vertical neutrinos).

While the  $\mu$  zenith angle distribution is very asymmetric,  $e$ -like events show no asymmetry.

The main result can be approximately extracted from very simple considerations, looking at the zenith-angle dependence of  $\mu$ -like multi-GeV data. Downward going neutrinos ( $\downarrow$ ) are almost unaffected by oscillations, while upward going neutrinos ( $\uparrow$ ) feel almost averaged oscillations, and therefore their flux is reduced by a factor  $1 - \frac{1}{2} \sin^2 2\theta_{\text{atm}}$ . This must be equal to the up/down ratio  $N_\uparrow/N_\downarrow = 0.5 \pm 0.05$ , so that  $\sin^2 2\theta_{\text{atm}} = 1 \pm 0.1$ . Furthermore, fig. ??? shows that multi-GeV neutrinos have energy  $E_\nu \sim 3$  GeV. According to fig. ???, they begin to oscillate around

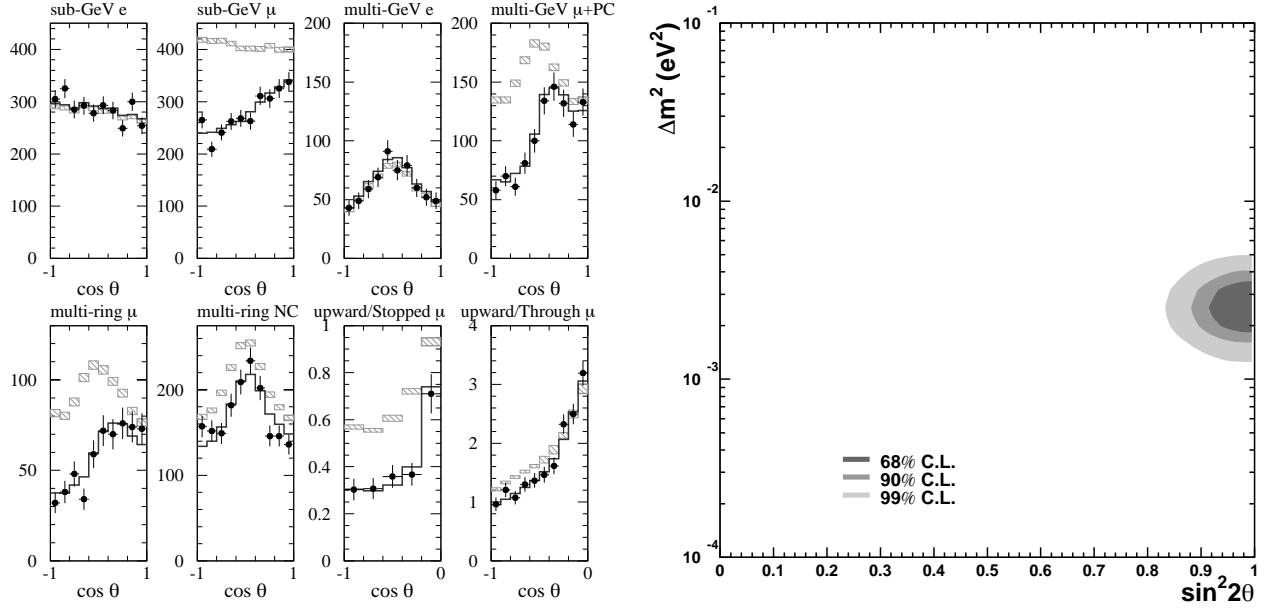


Figure 11: *SK data from Smy.*

the horizontal ( $\cos \vartheta \sim 0$ ) i.e. at a pathlength of about  $L \sim (hD_E) \sim 1000$  km. Therefore  $\Delta m_{\text{atm}}^2 \sim E_\nu/L \sim 3 \cdot 10^{-3} \text{ eV}^2$ .

Global fit add more less safe information. (the  $e/\mu$  ratio is now irrelevant, explain atm nu)

An important question is: *has SK probed the specific energy and pathlength dependence predicted by oscillations, eq. (5)?*

- Concerning the  $L$ -dependence, SK can see that  $P(\nu_\mu \rightarrow \nu_\mu)$  decreases by 50% when going from short to long baselines. However it cannot observe the most characteristic feature of oscillations: the first oscillation dip. As illustrated in fig. 4b at page 13, this happens because SK cannot measure the neutrino energy: the oscillation pattern gets washed when averaging over too different neutrino energies. Still the dip-less SK data in fig. 10 are in excellent agreement with the oscillation prediction. Fitting the SK data in terms of specific survival probability without oscillation dips, like

$$P(\nu_\mu \rightarrow \nu_\mu) = 1 - (\sin^2 \theta + \cos^2 \theta e^{-L/E\tau})^2 \quad \text{and} \quad \left| \cos^2 \theta + \sin^2 \theta (1 - \text{erf} \sqrt{\frac{icL}{E}}) \right|^2$$

(as suggested by decay of mixed neutrinos, and by mixing with extra dimensional neutrinos) one finds a  $\sim 4\sigma$  preference for the  $P(\nu_\mu \rightarrow \nu_\mu)$  predicted by  $\nu_\mu \rightarrow \nu_\tau$  oscillations [?].

- Concerning the  $E$ -dependence, oscillations predict that the atmospheric anomaly should disappear when the energy increases. This is indeed what SK finds, as illustrated in fig. ???. One can be more quantitative: fitting the SK data in terms of

$$P(\nu_\mu \rightarrow \nu_\mu) = 1 - \sin^2 2\theta \sin^2 \alpha L E^n$$

( $n = -1$  is predicted by oscillations;  $n = 0$  can be obtained from CPT violation;  $n = 1$  from violation of Lorentz invariance) one finds  $n = -1.03 \pm 0.13$  [4].

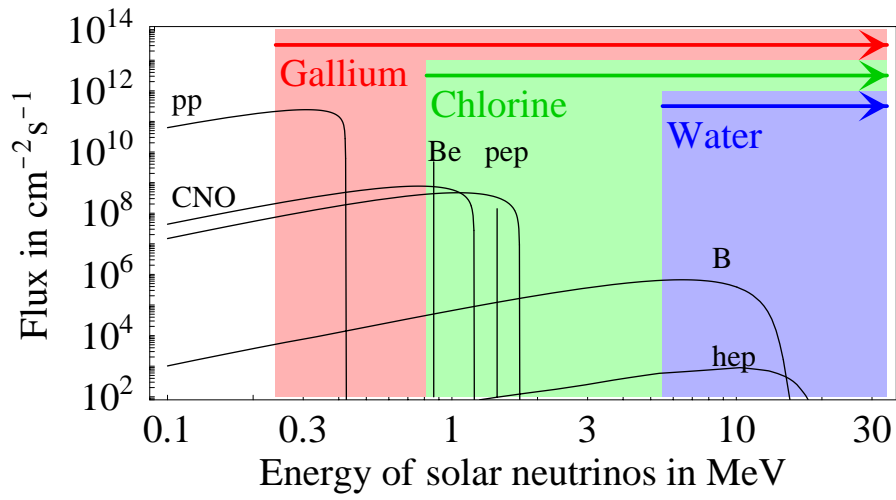


Figure 12: *The spectrum of solar neutrinos, together with the energy threshold of the different experiments performed so far.*

### 6.3 Bounds from reactor experiments: CHOOZ

### 6.4 Macro

### 6.5 K2K

## 7 The solar evidence

### 7.1 Solar neutrinos

Around the end of 19th century, after a careful study of the bible, European theologists (like XX) proclaimed that the earth had been created in 4096 B.C. Biologists and geologists (like Darwin) suggested that more than 300 Myr were necessary for natural selection and erosion. Physicists (like Kelvin) showed that, converting gravitational energy into thermal light, the sun can shine for  $GM^2/RK_\odot \sim 30$  Myr at most, emitting the flux of energy that we receive at earth,  $K_\odot = 8.53 \cdot 10^{11}$  MeV cm<sup>-2</sup> s<sup>-1</sup>.

Biologists and geologists were right. Physicists (like Aston, Eddington, Gamow, Bethe) later realized that the sun shines thanks to nuclear fusion. Around the center of the sun, energy and neutrinos are produced essentially through the reaction

$$4p + 2e \rightarrow {}^4\text{He} + 2\nu_e \quad (Q = 26.73 \text{ MeV}). \quad (21)$$

The typical neutrino energy is only few MeV: most of the energy is carried out from the sun by photons. Photons employ about  $10^4$  years to random-walk out of the solar interior and carry to the earth the well known flux of energy,  $K_\odot$ . Therefore, the present total neutrino luminosity of the sun is  $\Phi \sim 2K_\odot/Q \sim 6.4 \cdot 10^{10}/\text{cm}^2\text{s}$ .

The predicted neutrino spectrum, in absence of oscillations, is shown in fig. 12. The reason of such a complex spectrum is that the overall reaction (21) proceeds in a sequence of steps following different routes. The main routes are summarized in fig. 13, and give rise to five main types of neutrinos. The *pep* and Be neutrinos, generated by electrons colliding on heavy particles, are almost monochromatic.

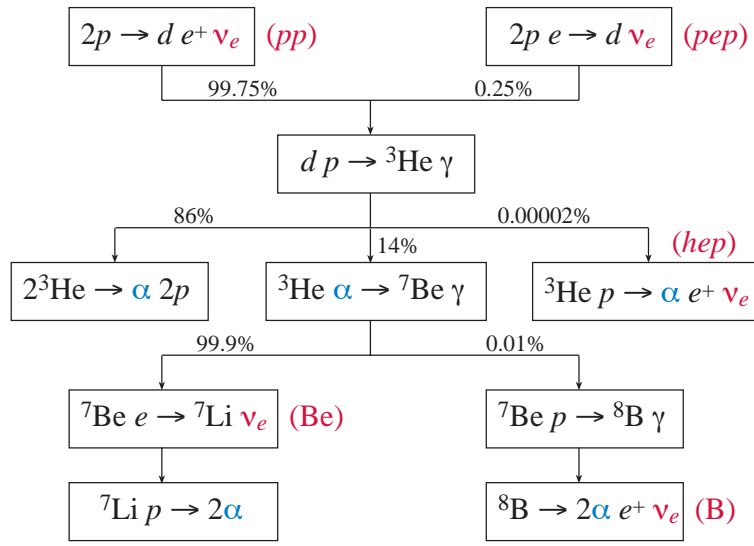


Figure 13: The  $4p + 2e \rightarrow {}^4\text{He} + 2\nu_e$  chain.

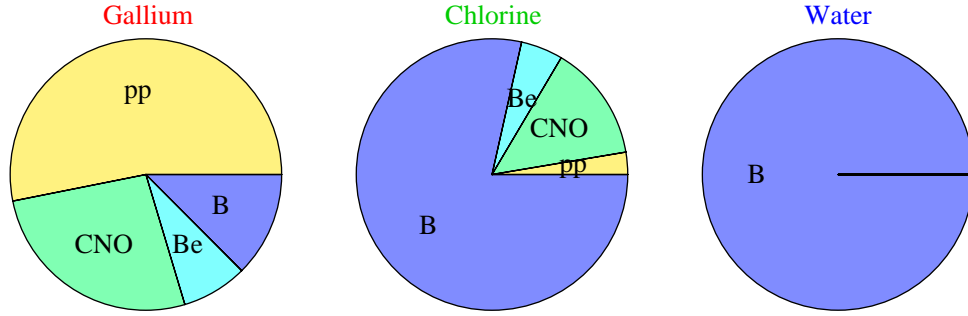


Figure 14: Fractional contributions to the neutrino rates of present experiments, assuming energy-independent oscillations.

1.  $pp$  neutrinos are the dominant component. They have a large and precisely predicted flux. However they have smaller energy, so that it is difficult to measure them.
2.  $pep$  neutrinos have a relatively small flux and low energy, but are not totally negligible.
3. Be neutrinos have a relatively well predicted and large flux and relatively high energy and are already important for present experiments, as shown in fig. 14. They are of great interest for future experiments, mainly because they are almost monochromatic,  $E_{\text{Be}} = m_{\text{Be}} - m_{\text{Li}} - m_e = 0.863 \text{ MeV}$ , allowing interesting measurements (see below).
4. B neutrinos are a very small fraction of all solar neutrinos, but their energy is high enough so that they can be precisely studied by SK and SNO.
5.  $hep$  neutrinos have the highest energy, but are too rare for having a significant effect, given the accuracy of present experiments.

Furthermore another chain CNO at solar temperatures

The energy spectra of the various components do not significantly depend on details of the solar interior, but are essentially determined by kinematics. Solar models play a crucial rôle in



predicting their total fluxes. The main uncertainties today are due to  $S_{17}$  (that parameterizes the  ${}^7\text{Be } p \rightarrow {}^8\text{B} \gamma$  cross-section of fig. 13, thereby fixing the total flux of B neutrinos) and to  $S_{34}$  (that parameterizes the  ${}^3\text{He } \alpha \rightarrow {}^7\text{Be} \gamma$  cross-section of fig. 13, thereby fixing the total flux of B plus Be neutrinos).

## 7.2 Fitting solar data

Fitting solar data is unfortunately a delicate job. Assuming that the solar anomaly is due to oscillations, one needs neutrino to compute propagation in the sun, in the space and in the earth (for neutrinos arrived during the night), taking into account matter effects in the sun and in the earth, and seasonal effects due to the excentricity of the earth orbit. One needs to average over the neutrino production point in the sun, as predicted by solar models, using the solar density profile predicted by solar models. Neutrinos produced around the center (on the opposite side) of the sun experience one (two) MSW resonances. Accurate semi-analytic approximations are available. One can now predict the rate measured by the various experiments, taking into account their energy thresholds. In order to extract the oscillation parameters from the data, one forms a global  $\chi^2$ , taking into account the correlated errors on the solar model predictions, on the cross sections, and the statistical and systematic experimental errors.

The result is shown in fig. ???. There are two main solutions, both with large mixing angle. The one with larger (lower)  $\Delta m^2$  is conventionally named ‘LMA’ (‘LOW’; its long tail below  $10^{-8} \text{ eV}^2$  is named ‘QVO’).

The main feature of the result can be understood in a simple way.

SK and SNO tell us that, at  $E_\nu \sim 10 \text{ MeV}$   $P_{ee}(E_\nu) \lesssim 1/2$  and is almost energy independent. This is sufficient to sigle out large mixing angle solutions: as illustrated in fig. ?? small mixing angle and VO solutions give an energy-dependent  $P_{ee}$  around  $P_{ee} \sim 1/2$ . SK also tells that matter effects in the earth are small:

$$A_{\text{DN}} = 2 \frac{N - D}{N + D} = ??$$

The neutrino energy at which earth matter effects induce a maximal day/night asymmetry is

$$E_\nu^{\text{res}} = \frac{\Delta m^2}{2\sqrt{2}G_F N_e^\oplus} \approx 2 \text{ MeV} \frac{\Delta m^2}{10^{-6} \text{ eV}^2},$$

where  $N_e^\oplus$  is the electron density of the earth mantle. This excludes values of  $\Delta m^2$  between the LMA and LOW solutions.

## 7.3 Bounds from reactor experiments: CHOOZ

## 7.4 Non standard solar fits

Non standard fits: rates vs sp d/n.

## 7.5 Towards the final solution

The relevant physics is quite different in these LMA, LOW and QVO regions. This gives rise to different signals that can be discovered by future experiments. KamLand, Borexino, sub-MeV

## LMA

Let us discuss t

A fully energy-independent  $P_{ee}(E_\nu)$  does not fit the data very well. LMA and LOW different small spectral distortions (LMA fits best the data but worse the spectra).

We now discuss how sub-MeV experiments could improve on this situation. Solar neutrinos with energy

$$E_\nu \lesssim \frac{\Delta m^2}{2\sqrt{2}G_F N_e^\odot} \approx 1 \text{ MeV} \frac{\Delta m^2}{10^{-5} \text{ eV}^2} \quad (22)$$

(where  $N_e^\odot$  is the electron density around the region of neutrino production) do not experience the MSW resonance in the sun. Therefore, their oscillation probability is roughly given by averaged vacuum oscillations,  $P_{ee} \approx 1 - \frac{1}{2} \sin^2 2\theta$ .

The survival probability of sub-MeV neutrinos is given by adiabatic conversion:  $P_{ee} = \sin^2 \theta$  during the day.

Indeed, in the QVO region the survival probability  $\langle P_{ee} \rangle = \frac{1}{2} + (P_C - \frac{1}{2}) \cos 2\theta$  lies somewhere between vacuum oscillations ( $\langle P_{ee} \rangle = 1 - \frac{1}{2} \sin^2 2\theta$  for  $P_C = \cos^2 \theta$ ) and adiabatic oscillations ( $\langle P_{ee} \rangle = \sin^2 \theta$  for  $P_C = 0$ ), as controlled by the crossing-probability  $P_C = [e^{\gamma \cos^2 \theta} - 1]/[e^\gamma - 1]$  where [?]

$$\gamma = \frac{\pi \Delta m^2}{E_\nu |d \ln N_e / dr|_{\text{res}}} \approx \frac{\Delta m^2 / E_\nu}{10^{-9} \text{ eV}^2 / \text{MeV}}.$$

The gradient is evaluated around the resonance point (for a more accurate approximation see [?]) where the density is  $N_e \sim \Delta m^2 / G_F E_\nu$ : this corresponds to the outer part of the sun where the profile density deviates from the simple exponential approximation,  $N_e \propto \exp(-10.54 r / R_{\text{sun}})$ .

## 8 The global oscillation picture?

We have discussed the two established neutrino anomalies. Few other anomalies, to be discussed in section 11, could be confirmed or refuted by future experiments. For the moment we ignore them and discuss how the solar and atmospheric data can be jointly explained in terms of oscillations between the three SM neutrinos. The  $\Delta m^2$  responsible of the atmospheric anomaly is larger, maybe much larger, than the one responsible of the solar anomaly. Therefore we identify

$$|\Delta m_{13}^2| \approx |\Delta m_{23}^2| = \Delta m_{\text{atm}}^2 \approx 3 \cdot 10^{-3} \text{ eV}^2, \quad \Delta m_{12}^2 = \Delta m_{\text{sun}}^2 \approx 10^{-(4 \div 10)} \text{ eV}^2.$$

As explained in section 3, the neutrino mixing matrix contains 3 mixing angles: two of them ( $\theta_{23}$  and  $\theta_{13}$ ) produce oscillations at the larger atmospheric frequency, one of them ( $\theta_{12}$ ) gives rise to oscillations at the smaller solar frequency. The CHOOZ constraint tells that  $\nu_e$  are can only be slightly involved in atmospheric oscillations, and SK agrees in explaining atmospheric data with  $\nu_\mu \rightarrow \nu_\tau$  transitions with large mixing angle. Solar data also want a large mixing angle. These considerations single out the global solution

$$\theta_{23} = \theta_{\text{atm}} \sim \pi/4 \quad \theta_{12} = \theta_{\text{sun}} \lesssim \pi/4, \quad \theta_{13} \sim 0, \quad \phi = \text{unknown}.$$

Nothing is known on the CP-violating phase  $\phi$ . If  $\theta_{13} = 0$  the solar and atmospheric anomalies depend on different set of parameters; there is no interplay between them. A  $\theta_{13} \neq 0$  would affect both solar and atmospheric data. Both data provide some upper bound on  $\theta_{13}$ , preferring  $\theta_{13} = 0$ . The strongest bound on  $\theta_{13}$  is directly provided by the CHOOZ experiment. In conclusion, all pieces of data point in the same direction, and can be analyzed without performing a 3 neutrino analysis.

## 8.1 What remains to be done?

We here *assume* that oscillations between the 3 SM neutrinos are the true global picture. While plausible, this is only an assumption to be tested by future experiments, that could discover something more, or something different. If our assumption is true, the goal of future experiments is the reconstruction of the neutrino mass matrix. Proceeding in steps, this means

1. Establishing oscillations.
2. Measuring better and better the solar and atmospheric parameters.
3. **Discovering the last mixing angle**,  $\theta_{13}$  that induces  $\nu_\mu \leftrightarrow \nu_e$  oscillations at the atmospheric frequency.

If a non zero  $\theta_{13}$  will be discovered...

4. Oscillations in matter allow to discriminate **the sign of  $\Delta m_{23}^2$**  [?] (i.e. if the atmospheric anomaly is due to the lightest or heaviest neutrinos, see fig. 3). If  $\Delta m_{23}^2 > 0$  (normal hierarchy) matter effects enhance  $\nu_\mu \leftrightarrow \nu_e$  oscillations and suppress  $\bar{\nu}_\mu \leftrightarrow \bar{\nu}_e$ , while the opposite happens if  $\Delta m_{23}^2 < 0$  (inverted hierarchy).
5. The **sign of  $\theta_{23} - 45^\circ$**  (which tells whether the neutrino state with mass  $m_3$  contains more  $\nu_\tau$  or more  $\nu_\mu$ ) can be measured by comparing

$$P(\nu_e \rightarrow \nu_e) = 1 - \sin^2 2\theta_{13} \sin^2 \frac{\Delta m_{23}^2 L}{4E_\nu} \quad \text{with} \quad P(\nu_\mu \rightarrow \nu_e) = \sin^2 \theta_{23} \cdot [1 - P(\nu_e \rightarrow \nu_e)]$$

Note that  $\nu_\mu$  disappearance experiments alone cannot distinguish  $\theta_{23}$  from  $90^\circ - \theta_{23}$ , and that the present bound  $\sin^2 2\theta_{23} \gtrsim 0.95$  [?] allows the relatively loose range  $1/3 \lesssim \sin^2 \theta_{23} \lesssim 2/3$ . If  $\Delta m_{12}^2$  is in the upper part of the LMA region, so that it affects long-baseline experiments, the sign of  $\theta_{23} - 45^\circ$  can be measured even if  $\theta_{13} = 0$ .

If a non zero  $\theta_{13}$  will be discovered and if  $\Delta m_{\text{sun}}^2$  lies in the LMA region

6. The **CP-violating phase  $\phi$**  can be measured in realistic long-baseline oscillation experiments.

Finally, oscillation experiments cannot access the whole neutrino mass matrix and cannot tell if neutrinos have Majorana or Dirac masses. Oscillations are sensitive to squared neutrino mass differences, but not to the overall scale of neutrino masses. We have measured the charged lepton Dirac masses  $m_e$ ,  $m_\mu$ ,  $m_\tau$ . It would be unsatisfactory if instead we knew only the values of  $m_\tau^2 - m_\mu^2$  and  $m_\mu^2 - m_e^2$ . In the Dirac case oscillation experiments miss only the overall neutrino mass scale. In the Majorana case they also miss two CP-violating phases,  $\alpha$  and  $\beta$ .

7. We need non oscillation experiments.

## 9 Future oscillation experiments

### 9.1 Atmospheric experiments

Monolith

## 9.2 Solar experiments

## 9.3 Reactor experiments

Per  $\theta_{13}$ .

## 9.4 Neutrino beams

There is 1 established technique, and some proposal

**Conventional beam** *da Andrea*: La formula a 3 neutrini con materia e  $\text{dmm}21 = 0$  si ottiene da quella a 3 neutrini senza materia nel limite  $\text{dmm}21 = 0$  aggiungendo gli effetti di materia come si farebbe in un sistema a 2 neutrini con  $\text{dmm} = \text{dmm}32$  e  $\text{theta} = \text{theta}13$  (la rotazione 12 e la fase non sono fisiche e la rotazione 23 commuta con l'effetto di materia per cui uno ha ad esempio la formula 25 di 9912457). Also 0004085.

## 9.5 Superbeam

## 9.6 Neutrino factory

# 10 Non oscillation experiments

No effect has been seen so far, but experiments seem not far from reaching the necessary sensitivity.

## 10.1 $\beta$ -decay

One way to search for neutrino masses (more specifically for a  $\bar{\nu}_e$  mass) is to measure the electron spectrum in the  $\beta$ -decay of a nucleus (i.e.  $d \rightarrow ue\bar{\nu}_e$  at the quark level, and  $n \rightarrow pe\bar{\nu}_e$  at the nucleon level, fig. 15a). The most sensitive choice is tritium decay

$${}^3\text{H} \rightarrow {}^3\text{He} e \bar{\nu}_e \quad (Q = m_{{}^3\text{H}} - m_{{}^3\text{He}} = 18.6 \text{ keV}).$$

Energy conservation tells that  $E_e \simeq Q - E_\nu$ . More precisely, around the end-point  $E_e \sim Q - m_\nu$ , the energy spectrum is essentially determined by the neutrino phase space factor  $\propto E_\nu p_\nu$ . So

$$\frac{dN}{dE_e} = F(E_e)(Q - E_\nu)\sqrt{(Q - E_e)^2 - m_\nu^2}$$

where  $F(E_e)$  can be considered as a constant. The fraction of events in the end-point tail is  $\propto (m_\nu/Q)^3$ , so nuclear decays with a low  $Q$  (and a reasonable life-time) offer the best sensitivity. Older experiments found a  $4.6\sigma$  evidence for a negative  $m_\nu^2 = -96 \pm 21 \text{ eV}^2$  (probably because the energy resolution was overestimated), not confirmed by the most recent experiments TROITSK and MAINZ, that put the bound  $m_\nu < 2.2 \text{ eV}$  at 95% CL. Next generation experiments could improve the sensitivity by one order of magnitude.

If one does not trust CPT, a looser bound on  $m_{\nu_e} < 200 \text{ eV}$ . Experimentally tested cosmology requires  $\sum m_\nu \lesssim 50 \text{ eV}$ .

Bounds on  $\mu$  and  $\tau$  masses can be obtained studying decay like  $\pi \rightarrow \mu \bar{\nu}_\mu$ . The resulting bounds,  $m_{\nu_{\mu,\tau}} \lesssim \text{MeV}$  are very loose.

## 10.2 Neutrino-less double $\beta$ decay

Few nuclei can only decay through double  $\beta$ -decay. This is e.g. the case of  $^{76}_{32}\text{Ge}$ , that cannot  $\beta$ -decay to  $^{76}_{33}\text{As}$  that is heavier. It can only jump to the lighter  $^{76}_{34}\text{Se}$ :

$$^{76}\text{Ge} \rightarrow ^{76}\text{Se} ee \bar{\nu}_e \bar{\nu}_e \quad (Q = 2038.6 \text{ keV})$$

Since it is a second order weak process,  $^{76}\text{Ge}$  has a very long life-time,  $\tau \sim 10^{21}$  yr. If neutrinos have Majorana masses, the alternative neutrino-less double  $\beta$  decay ( $0\nu 2\beta$ ) decay  $^{76}\text{Ge} \rightarrow ^{76}\text{Se} ee$  is also possible (fig. 15b). The decay amplitude is proportional to  $m_{ee}$ , the  $\nu_{eL}\nu_{eL}$  element of the neutrino mass matrix. The experimental signal is: two electrons with total energy equal to  $Q$  (while  $2\beta$  decay gives two electrons with total energy equal or less than  $Q$ ). HEIDELBERG-MOSCOW finds  $\tau \gtrsim 10^{25}$  yr that corresponds to  $|m_{ee}| < 0.38h$  eV at 95% CL, where  $h \sim 1$  remembers that there is a  $\sim 50\%$  theoretical uncertainty on the relevant nuclear matrix element.

## 11 Unconfirmed anomalies

### 11.1 LSND

Both in the LSND and Karmen experiments, a proton beam is used to produce  $\pi^+$ , that decay as

$$\pi^+ \rightarrow \mu^+ \nu_\mu, \quad \mu^+ \rightarrow e^+ \nu_e \bar{\nu}_\mu$$

generating  $\bar{\nu}_\mu, \nu_\mu$  and  $\nu_e$  neutrinos. The resulting neutrino beam also contains a small  $\bar{\nu}_e$  contamination, about  $\bar{\nu}_e/\bar{\nu}_\mu \lesssim 10^{-3}$ .

The search for  $\bar{\nu}_\mu \rightarrow \bar{\nu}_e$  is performed using the detection reaction  $\bar{\nu}_\mu p \rightarrow n e^+$ , that has a large cross section. The detector tries to identify both the  $e^+$  and the  $n$  (via the 2.2 MeV  $\gamma$  line obtained when  $n$  is captured by a proton). The neutrino beam has energy  $E_\nu \sim (10 \div 50)$  MeV and travels for  $L \approx 30$  m in LSND and  $L \approx 17.5$  m in Karmen. These experiments are more sensitive to oscillations than older experiments, that used higher neutrino energy.

LSND finds an evidence for  $\bar{\nu}_\mu \rightarrow \bar{\nu}_e$ , that ranges between 3 to  $7\sigma$  depending on how data are analyzed. This happens because LSND has a poor signal/background ratio: choosing the selection cuts as in [?] the LSND sample contains 1000 background events and less than 100 signal events, distinguished only on a statistical basis. The main backgrounds are cosmic rays and  $\nu_e$  misidentification.

Karmen finds 15 events versus an expected background of 15.8 events. Karmen has a few times less statistics and shorter base-line than LSND, but is much cleaner. The main reason is that the Karmen beam is pulsed, allowing to reduce the cosmic ray background (Karmen also has a better shield), and also  $\nu_e$  misidentification (due to a nuclear decay with a life-time different than the one characteristic of  $n$  capture). At the end, Karmen excludes a significant part, but not all, of the  $(\Delta m^2, \theta)$  range suggested by LSND.

The LSND anomaly will be tested by the MiniBoone experiment, that will have more statistics than LSND and a pulsed beam. Initially, MiniBoone will look for  $\nu_\mu \rightarrow \nu_e$ .

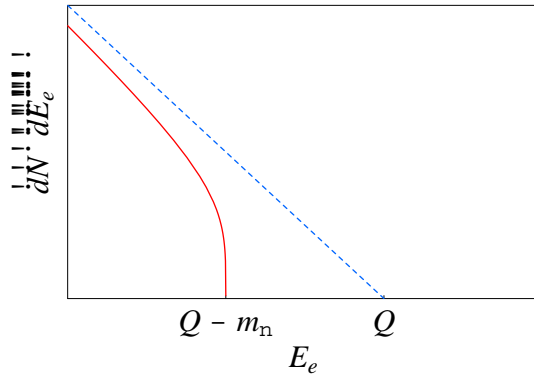


Figure 15: *Fig. 15a:  $\beta$ -decay spectrum close to end-point for a massless (dotted) and massive (continuous line) neutrino. Fig. 15b:  $2\beta$  and  $0\nu 2\beta$  spectra.*

**Sterile neutrinos?**

$\mu$  decay?

## 11.2 NuTeV

## 11.3 Heidelberg-Moscow

also 1948 E. Fireman

## 11.4 Ultra-high energy cosmic rays

# 12 Supernovæ

At 7:36 (UT) of 23 february 1987 neutrinos emitted in the collapse of a star in the Magellanic cloud (170000 light years from us) arrived at the earth and were detected by experiments built to search for proton decay: KamiokandeII (12 events), IMB (8 events) and Baksan (6 events).

In subsection 12.1 we explain the basic physics of supernovæ, in order to understand why and how they emit neutrinos. The uninterested reader can jump to subsection 12.2, where we summarize the results and discuss their implications for neutrino masses and oscillations. At the moment there are no safe and interesting implications: the very uninterested reader might want to skip all this section. .

## 12.1 What a supernova is

Neglecting order-one factors, we now discuss what happens to a star of mass  $M$  and radius  $R$ , volume  $V \sim R^3$ , composed by  $N = M/m_n \sim 10^{57} M/M_{\text{sun}}$  nucleons (with mass  $m_n$ ) and  $\sim N$  electrons (with mass  $m_e$ ), with density  $\rho \sim M/R^3$  and number density  $n = N/V = \rho/m_n$ . A single particle occupies an average volume  $v \sim R^3/N$  and has energy  $u$ .

A large enough cloud of particles is unstable under gravity. The cloud contracts and the gravitational potential energy gets converted into kinetic energy,  $Nu = GM^2/R$ , heating the gas. If the mass is large enough, the gas becomes hot enough and the nuclear reaction (21) begins to burn hydrogen into helium. The nuclear energy stops the contraction: one gets a star that can shine for some time. When hydrogen is finished, the star contracts and heats again, up to when

is becomes sufficiently hot to burn helium into carbon. After few of these steps one has an inert iron core, that cannot burn any more because  $^{56}\text{Fe}$  is the most bound of all nuclei. The core is surrounded by shells of unburned lighter nuclei.

At this point, different things may happen, depending on the mass of the star. It remains stable if the force due to pressure ( $F \sim pR^2$ ) compensates the attractive force due to gravity ( $F \sim GM^2/R^2$ ) i.e. if  $p = GM^2/R^4$ . Assuming an equation of state  $p(\rho)$  of the form  $p \propto \rho^\gamma$ , stability is possible for  $\gamma > 4/3$ . The quantum pressure becomes the dominant pressure within the dense core, and may be or may be not enough to keep the star stable.

Since Fermi particles obey the Pauli exclusion principle, the uncertainty principle  $\Delta x \Delta p \sim \hbar$  implies that, even at zero temperature, fermions have a minimal Fermi momentum:  $p_F \sim \hbar n^{1/3}$  where  $n = N/V$ .<sup>9</sup> Non-relativistic electrons have an energy  $u = p_F^2/2m_e \sim n^{2/3}\hbar^2/m_e$ . Remembering law  $pV = n_{\text{molar}}RT$ , the Fermi pressure is

$$p \sim \frac{u}{v} = \frac{uN}{V} \sim n^{5/3} \frac{\hbar^2}{m_e} = K\rho^{5/3} \quad \text{where} \quad K \sim \frac{\hbar^2}{m_e m_N^{5/3}}$$

The quantum pressure of the other heavier particles that dominate the mass density is negligible: they have smaller Compton wavelength than electrons, so that their quantum effects are negligible. A non-relativistic Fermi electron gas has  $\gamma = 5/3$  and therefore supports gravitational compression, giving rise to a ‘white dwarf’.

However, electrons become relativistic if the star is heavier than the Chandrasekhar mass limit,  $M \gtrsim M_{\text{Ch}} \sim (\hbar c/G)^{3/2}/m_n^2$ . Including order one factors,  $M_{\text{Ch}} = 1.4M_{\text{sun}}$ . The energy of relativistic electrons is  $u \sim cp_F \sim \hbar n^{4/3}$  and their Fermi pressure becomes  $p \sim \hbar n^{4/3} = K\rho^{4/3}$  with  $K = \hbar/m_n^{4/3}$ . An ultra-relativistic Fermi electron gas has  $\gamma = 4/3$ : if  $M \gtrsim M_{\text{Ch}}$  the star collapses and becomes so hot that photons and electrons break the iron nuclei. Inverse nuclear fusion subtracts thermal energy (thereby reducing the pressure and accelerating the collapse) that escapes as  $\nu_e$  generated via the  $ep \rightarrow n\nu_e$  process. This is named ‘deleptonization burst’ since during this stage  $\nu_e$  carry away not only some small fraction of the total energy (simulations suggest few %), but also almost all lepton number. After few ms, in the core remain the neutrons (that carry the conserved baryon number) plus a particle/antiparticle sea at an increasing temperature  $T \gg m_e$ . The particles lighter than  $T$  are photons, electrons, eventually muons, and all kind of neutrinos (produced by CC and NC scatterings).

When the core reaches nuclear density, the collapse gets halted by the quantum pressure of neutrons, that are non relativistic and therefore have  $\gamma = 5/3$ , giving rise at least to a partial rebound that generates the light that we can see. If also neutrons become ultra-relativistic,  $T \gg m_n$ , their equation of state is the standard one,  $p = \frac{1}{3}\rho$ . The value  $\gamma = 1$  can be obtained adapting the estimate done for electrons, taking into account that now  $\rho = un$ , rather than  $\rho = m_n n$ . The eventually ultra-relativistic neutrons collapse into a black hole. However nobody knows what happens when  $T \sim m_n$ , because nobody can solve non perturbative QCD.

We can now discuss what happens to neutrinos. When collapsing from atomic density (one particle per Angstrom<sup>3</sup>) to nuclear density (one particle per Fermi<sup>3</sup>  $\sim 1/\text{GeV}^3$ ) the core becomes  $10^5$  times smaller, so that its typical radius is few km. An enormous amount of gravitational energy gets converted into kinetic energy

$$E_{\text{tot}} = \frac{GM_{\text{core}}^2}{R_{\text{core}}} = 5 \cdot 10^{53} \text{ erg} \frac{M_{\text{core}}^2/M_{\text{Ch}}^2}{R_{\text{core}}/10 \text{ km}}, \quad u = \frac{E_{\text{tot}}}{N} = 200 \text{ MeV} \cdot \frac{M_{\text{core}}/M_{\text{Ch}}}{R_{\text{core}}/10 \text{ km}}.$$

---

<sup>9</sup>Although we use natural units, we write  $\hbar$  and  $c$  factors when this makes the physics more transparent.



The total energy is  $\sim 4m_n/Q \sim$  few hundred times larger than the total energy that the sun emits burning for  $10^{10}$ yr according to the reaction (21). The core is so dense that neutrinos are efficiently produced and partly trapped (while photons are too strongly trapped, and gravitons are so weakly coupled that are neither trapped nor produced with a significant abundance<sup>10</sup>). Since the neutrino cross section is  $\sigma \sim G_F^2 E_\nu^2$  and the particle number density is  $n \sim T^3$ , the neutrino mean free path is  $\ell \sim 1/n\sigma \sim 1/(G_F^2 T^5) \sim 10 \text{ km} (10 \text{ MeV}/T)^5$ . This means that neutrinos random walk in the interior and only escape when they reach the outer and cooler part of the supernova (named ‘neutrinosphere’). Neutrinos are predicted to have a thermal spectrum with temperature of about 10 MeV. Since neutrinos are partially trapped they need few seconds to carry out all energy. Different neutrinos are trapped by different reactions [ $\bar{\nu}_e n$ ,  $\nu_e p$ ,  $\nu_{\mu,\tau} N$  There are more  $n$  than  $p$ ]

$$\sigma(\bar{\nu}_e) > \sigma(\nu_e) > \sigma(\nu_\mu, \nu_\tau, \bar{\nu}_\mu, \bar{\nu}_\tau)$$

so that  $\bar{\nu}_e$  are emitted with a lower temperature than the other neutrinos.

## 12.2 Supernovæ and neutrinos

We summarize the previous subsection. There are two main components of the neutrino flux emitted by a supernova. During the first few milliseconds,  $10^{57} \nu_e$  of energy  $\sim 10 \text{ MeV}$  freely escape carrying away the lepton number of the star and  $\sim 10\%$  of the total energy. The collapse goes on, converting gravitational energy into thermal energy, that is almost entirely radiated by the weakly trapped neutrinos. These neutrinos have a Fermi-Dirac spectrum, so that temperature and average energy are related as  $T = \langle E \rangle 180 \zeta(3)/7\pi^4 \approx \langle E \rangle / \pi$ . Detailed simulations suggest that, for SN1987 in absence of oscillations

$$\langle E_{\bar{\nu}_e} \rangle \sim 15 \text{ MeV}, \quad \langle E_{\nu_e} \rangle \sim 12 \text{ MeV}, \quad \langle E_{\bar{\nu}_{\mu,\tau}, \nu_{\mu,\tau}} \rangle \sim 25 \text{ MeV}, \quad E_{\text{tot}} \sim 3 \cdot 10^{53} \text{ erg}$$

but cannot tell how accurate are these predictions.

The WČ experiments KamiokandeII and IMB detected the  $\bar{\nu}_e$ . In fact, the reaction  $\bar{\nu}_e p \rightarrow n e^+$  has a cross section  $\sim 100$  larger than the cross section of the other  $\nu$  and  $\bar{\nu}$ . Furthermore it gives  $e^+$  with almost isotropic angular distribution (in contrast with the forward-peaked reaction  $\nu_e e \rightarrow \nu_e e$ ), in agreement with data. The few observed events were detected in a dozen of seconds, in rough agreement with the expected cooling time of SN1987A.

These data have few interesting implications:

- One immediate consequence is that  $\bar{\nu}_e$  are lighter than about 20 eV, otherwise the difference in time-of-flight ( $t \simeq D + Dm_\nu^2/2E_\nu^2$ : less energetic neutrinos are slower) between  $\bar{\nu}_e$  of different energy exceeds the observed duration of the pulse. Data at a future supernova will allow to improve this bound, but not at a level competitive with direct bounds on neutrino masses (section 10).
- The  $\bar{\nu}_e$  life-time is longer than  $\tau_\nu \gtrsim 170000 \text{ yr} \times m_\nu/E_\nu < 10^4 \text{ s}$ . Together with CPT-invariance, this implies that  $\nu_e$  decay cannot explain the solar neutrino anomaly.
- magnetic moment
- Extra particles, right-handed neutrinos

---

<sup>10</sup>Experiments will try to detect the gravity waves in the near future.

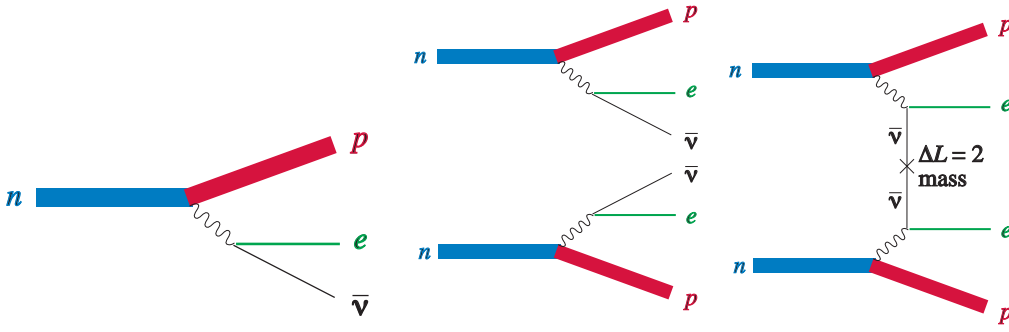


Figure 16:  $\beta$  decay, double  $\beta$  decay, and neutrino-less double  $\beta$  decay.

- If supernovæ simulations are correct, SN1987A data disfavour oscillations solar oscillations with large mixing angle and atmospheric oscillations with  $\theta_{13} \gtrsim 1^\circ$  and  $\Delta m_{23}^2 < 0$  ('inverted' spectrum).

In fact, the average  $\bar{\nu}_e$  energy deduced from KamiokandeII and IMB data is  $\langle E_{\bar{\nu}_e} \rangle \sim 11$  MeV, assuming the overall  $E_{\text{tot}}$  suggested by supernova simulations (experimental data alone do not allow to extract both quantities accurately). This is somehow smaller than the value suggested by supernova simulations in absence of oscillations,  $E_{\bar{\nu}_e} \sim 15$  MeV. For both figures it is difficult to properly assign errors; but oscillations that convert  $\bar{\nu}_e \leftrightarrow \bar{\nu}_{\mu,\tau}$  increase the disagreement, since supernova simulations suggest  $\langle E_{\bar{\nu}_{\mu,\tau}} \rangle \sim 25$  MeV. With an inverted hierarchy,  $\theta_{13} \gtrsim 1^\circ$  gives rise to adiabatic MSW conversion, swapping  $\bar{\nu}_e \leftrightarrow \bar{\nu}_{\mu,\tau}$  completely (the adiabaticity parameter is  $\gamma \sim$ ). This is why this case is 'disfavoured' if the predictions of supernova models on neutrino energy and flux are correct. The same argument applies to large solar mixing angles:  $\theta_{12} \sim 1$  induces a partial swap of the  $\bar{\nu}_e$  into  $\bar{\nu}_{\mu,\tau}$ , whatever the mass spectrum of neutrinos. LMA oscillations have a smaller  $\theta_{12}$  and a larger  $\Delta m_{12}^2$  than LOW and (Q)VO, and are therefore less 'disfavoured'. SMA gives almost no  $\bar{\nu}_e$  oscillations, but is strongly disfavoured by solar data.

## 12.3 Oscillations

# 13 Understanding flavour

We measure quark, lepton and neutrino masses and mixings with the goal of sooner or later understanding why they are what they are. We will briefly review what has been done. In our opinion, we are not (yet) understanding flavour. If we hope doing better it is useful to recognize the limitations of the present approaches. [Strategia generale. Goal is trying to reconstruct some pattern. Could be U(1) charges or wave functions in extra dimensions; the problem is that...]

Lagrangian parameters receive divergent quantum correction. Without knowing what is the physical cut-off the only practicable way to get some control over the parameters is recognizing possible symmetries that relate different parameters. Few examples:

- Around 1970, thanks to **gauge invariance**, theorists were very useful in understanding experiments and in establishing the SM along the following road:

$$\text{photon} \rightarrow \text{gauge invariance} \rightarrow \text{gluons, } Z, W.$$

The most generic gauge invariant renormalizable Lagrangian that can be written with the SM fields contains 18 apparently fundamental parameters; 13 of them describe flavour. We

now have more than 13 experiments, that performed non trivial tests (no electric dipole moments, no  $\mu \rightarrow e\gamma$ ,  $\epsilon_K$ ,  $\epsilon'_K$ ,  $\Delta m_B$ ,  $b \rightarrow s\gamma$ ) and agree with SM predictions, disfavouring alternative models with a different flavour structure<sup>11</sup>.

- **Supersymmetry** could become another predictive symmetry, if it exists and is not broken at too high energy.
- In **SU(5) models** the 3 SM gauge couplings are rewritten in terms of 2 main parameters (the SU(5) gauge coupling, and the scale of SU(5)-breaking), giving one prediction. This is the most interesting result (maybe the only one) of beyond-the-SM theoretical physics.

Unfortunately, lepton and quark masses and mixings show no clear pattern that indicates the eventual symmetry behind them, and are still described by a list of 13 mysterious numbers.

It is hard to obtain predictions because flavour extensions of the SM involve many more unknown parameters. For example, neglecting neutrino masses, the  $3 \times 3$  lepton Yukawa matrix is described by 18 real parameters, but only 3 of them are measurable at low energy:  $m_e$ ,  $m_\mu$  and  $m_\tau$ . Since  $3 \ll 18$ , even very restrictive symmetries or assumptions do not succeed in giving testable predictions. In many different ways (e.g. postulating a broken U(1) flavour symmetry) it is possible to reproduce the hierarchy  $m_e \ll m_\mu \ll m_\tau$  (and the similar one in quarks) in terms of a small symmetry-breaking parameter and dozens of unknown order-one parameters. These efforts resulted in thousands of theoretical papers (one every few days since many years) with no observable consequence, with rare exceptions. To show just one example, the relatively more interesting attempt was assuming a texture of the form

$$\lambda_{U,D} = \dots$$

(eventually justifiable postulating e.g. a properly broken U(2) flavour symmetry) that leads to

$$V_{?} = \sqrt{\frac{m_d}{m_s}} + e^{i\phi} \sqrt{\frac{m_u}{m_c}}$$

However the resulting prediction for some CKM parameters has been contradicted by latest more accurate measurements.

Furthermore, the two large mixing angles implied by solar and atmospheric neutrino anomalies (assuming that they are due to oscillations) contradicted previous theoretical predictions/expectations/guesses. At the moment it is not clear which unexpected pattern is emerging from neutrino data. Three possibilities that could be selected by future data are:

1. **Mass hierarchy between largely mixed states:**  $\Delta m_{\text{sun}}^2 \ll \Delta m_{\text{atm}}^2$  and  $\theta_{\text{atm}} \sim 1$ . If true, would be a strong indication. While it is easy to obtain hierarchical masses with small mixing, or large mixing without mass hierarchies, only few Majorana neutrino mass matrices give both.
2. **Special values.**  $\theta_{\text{atm}} \simeq \pi/4$  or  $\tan^2 \theta_{\text{sun}} \simeq 1/2$  or  $\theta_{13} \simeq \sqrt{m_e/2m_\mu}$ . If mixing angles had these or other peculiar values, they would point towards some ‘big’ (non-abelian?) flavour symmetry.

---

<sup>11</sup>The SM has a U(3)<sup>5</sup> flavour symmetry broken only by the Yukawa couplings. This implies a peculiar strong suppression of CP-violating effects in  $K$  mixing and decay, and a very strong suppression of  $e, n$  electric dipoles, in agreement with present data.

3. **Nothing.** A neutrino mass matrix with generic  $\mathcal{O}(0.05)$  eV entries roughly corresponds to what we observe, if  $\theta_{13}$  is just below the present bound, and  $\Delta m_{\text{sun}}^2$  lies in the upper part of the LMA region. If true, indicates that lepton doublets are not charged under any flavour symmetry. Long-baseline and  $0\nu 2\beta$  experiments will measure more parameters, but we will not understand what they mean.

On 2. and 3. there is nothing to be said, so we now focus on 1., considering the different possible kinds of neutrino mass spectra.

### 13.1 Normal hierarchy

Could another origin. Renormalizable: seesaw or triplet.

Regole U(1)

**Normal hierarchy** The simplest way to justify large mixing angle is  $q_{L\mu} = q_{L\tau}$  (accidentally not large solar mixing).

## 14 Extras

### 14.1 RGE effects

We begin with the MSSM because is trivial. According to the non-renormalization theorem, only kinetic terms receive quantum corrections. Superpotential interactions (right-handed neutrino masses, their Yukawa couplings, and  $(LH)^2$ ) do not receive quantum corrections.

$$Z_{L_i L_j} = 1 - g^2 - \lambda_i \lambda_j \dots$$

(can be RGE resummed)

$Z_N$  is irrelevant,  $Z_H$  is just an overall rescaling.

### 14.2 Lepton-flavour violation from supersymmetry

A very unpleasant feature of the see-saw mechanism is that we do not see how it can be realistically tested, i.e. how it could became true physics rather than remaining a nice speculation.

In general, if the observed solar and atmospheric anomalies are due to neutrino masses, they imply lepton-flavour-violating (LFV) decays such as  $\mu \rightarrow e\gamma$  and  $\tau \rightarrow \mu\gamma$ . However the resulting rates are of order  $\text{BR}(\mu \rightarrow e\gamma) \sim (m_\mu m_{e\mu}/m_W^2)^2 \sim 10^{-50}$  (where  $m_{e\mu}$  is the  $e\mu$  element of the neutrino mass matrix) i.e. much below the present experimental bound  $\text{BR}(\mu \rightarrow e\gamma) < 10^{-11}$  and any possible future improvement. The electric dipole moment (EDM) of the electron,  $d_e$ , is even more strongly suppressed.

The same thing is true in see-saw models. The observed neutrino masses,  $m_\nu \sim \lambda_N^2 v^2/M_N$ , suggest that it will be impossible to observe the right-handed neutrinos, either because  $M_N$  is too heavy, or because  $\lambda_N$  is too small. The  $\mu \rightarrow e\gamma$  decay amplitude is again proportional to  $\lambda_N^2/M_N \propto m_\nu$ , i.e. is unobservably small.

If supersymmetric particles exists at the weak scale, things can be very different. In the context of the Minimal Supersymmetric Standard Model (MSSM) radiative corrections induced by  $\lambda_N$

affect supersymmetry-breaking slepton mass terms, if they are already present in the Lagrangian at energies above  $M_N$  (alternatively supersymmetry-breaking could instead be transmitted to MSSM particles at energies below  $M_N$ , where right-handed neutrinos no longer exist). The crucial difference between the SM and the MSSM is that the SM remembers of the existence of very heavy right-handed neutrinos only through non-renormalizable operators like  $(LH)^2/\Lambda$  (that give rise to neutrino masses). The MSSM contains more renormalizable terms, like slepton masses  $m_L^2 \tilde{L}^* \tilde{L}$ , where right-handed neutrinos can leave their imprint. For example, the correction to the  $3 \times 3$  mass matrix of left-handed sleptons is

$$m_L^2 = m_0^2 \mathbb{I} - \frac{3m_0^2}{(4\pi)^2} \mathbf{Y}_N + \dots \quad \text{where} \quad \mathbf{Y}_N \equiv \boldsymbol{\lambda}_N^* \ln\left(\frac{M_{\text{GUT}}^2}{\mathbf{M}\mathbf{M}^\dagger}\right) \boldsymbol{\lambda}_N^T \quad (23)$$

having assumed<sup>12</sup> universal soft terms at  $M_{\text{GUT}}$  and neglected  $A$ -terms and  $\mathcal{O}(\lambda_N^4)$  effects. In this approximation, the experimental bounds from  $\ell_i \rightarrow \ell_j \gamma$  decays are saturated for

$$[\mathbf{Y}_N]_{\tau\mu}, [\mathbf{Y}_N]_{\tau e} \sim 10^{1\pm 1}, \quad [\mathbf{Y}_N]_{\mu e} \sim 10^{-1\pm 1} \quad (24)$$

The precise value depends on the unknown sparticle spectrum, but it is pointless to make precise computations. Large neutrino couplings (e.g.  $\lambda_N \sim \lambda_t$ ) could give  $\mu \rightarrow e\gamma$  or  $\tau \rightarrow \mu\gamma$  just below their experimental bounds, while smaller neutrino couplings (e.g.  $\lambda_\nu \sim \lambda_\tau$ ) would give no significant effect. However, we have no idea of which value  $Y_N \sim \lambda_N^2$  should have (neutrino masses only tell us the value of  $\lambda_N^2/M_N$ ), so that *see-saw models make no testable prediction*. In fact, the  $\mathbf{M}_N, \boldsymbol{\lambda}_N$  and  $\boldsymbol{\lambda}_E$  matrices that describe the supersymmetric see-saw contain 15 real parameters and 6 CP-violating phases. At low energy, in the mass eigenstate basis of the leptons, 3 real parameters describe the lepton masses, and both the neutrino and the left-handed slepton mass matrices are described by 6 real parameters and 3 CP-violating phases. Since  $(15+6) = (3+0) + (6+3) + (6+3)$  we see that see-saw mechanism has too many free parameters to allow predictions: any pattern of lepton and neutrino masses is compatible with any pattern of radiatively-generated flavor violations in left-handed slepton masses.

### 14.3 Connection with supersymmetric unification

Neutrino data contradicted the simplest pattern suggested by supersymmetric unification

- **The expectation.** As suggested by GUT, neutrino masses arise from the see-saw mechanism, with neutrino Yukawa couplings comparable to the other Yukawa couplings. Therefore neutrinos have small mixing angles. With  $\theta_{e\mu} \sim (m_e/m_\mu)^{1/2}$  the deficit of solar  $\nu_e$  is nicely produced by resonant MSW effects. See-saw naturally gives small neutrino masses roughly proportional to squared quark (or lepton) masses:  $m_{\nu_\ell} \propto m_\ell^2$ . Since  $m_{\nu_\mu}^2 = \Delta m_{\text{sun}}^2$ ,  $\tau$ -neutrinos have eV masses, providing the hot dark matter suggested by cosmology. Kamiokande was designed to look for proton decay, as predicted by GUT ('nde' = nucleon decay experiment at the Kamioka mine).
- **The data.** NOMAD and CHORUS (designed to discover  $\nu_\mu \leftrightarrow \nu_\tau$  oscillations with large  $\Delta m^2$  and small mixing angle) found nothing, and cosmologists discovered that hot dark matter

---

<sup>12</sup>In the MSSM lepton flavour is not an accidental symmetry as in the SM, and some mechanism is supposed to suppress lepton/slepton mixing down to an acceptable level. This problem motivates the assumption of universal soft-terms at  $M_{\text{GUT}}$ , although nothing guarantees it. Rather, in GUT models the unified top quark Yukawa coupling distorts universal soft terms, imprinting sizable other LFV effects in them.

was not necessary. (Super)Kamio*kande* excluded the solar SMA solution and discovered  $\nu_\mu \leftrightarrow \nu_\tau$  oscillations with large mixing angle and small  $\Delta m^2$  ('*ande*' = atmospheric neutrino detector experiment).

SUSY GUT do not marry happily with neutrino masses. Infact if lepton number is not an exact symmetry, in SUSY models one generically expects heavy neutrinos: unlike in the SM  $L$ -violating effects remain at the weak scale. One possibility: 126 in SO(10) gives  $\Delta L = 2$ . Or matter parity.

bottom/tau unification...

## 14.4 Baryogenesys through leptogenesis

We observe that our universe contains mostly photons, a similar number of  $p$ ,  $n$ ,  $e$ , and almost no antiparticles (we do not know how many  $\nu$  and  $\bar{\nu}$  there are). The observed equality between  $e$  and  $p$  just means that there is no net electric charge. We also understand why the observed  $n/p$  ratio is  $\sim 1/7$ . This happens because free neutrons have a life time of about 10 minutes, and because  $\sim 3$  minutes after big-bang the universe becomes sufficiently cold that neutrons get bound in nuclei. The relative abundances of light nuclei are understood in the same way ('nucleosynthesis').

We do not understand why the observed amount of matter is  $n_B/n_\gamma \sim 6 \cdot 10^{-10}$ . . Such a value of  $n_B$  was implied by nucleosynthesis and was recently confirmed by observations of CMB anisotropies (specifically, the height of the second acoustic peak).

If the universe started with  $n_B = 0$  matter can be generated in the subsequent evolution if 1)  $B$  is violated; 2) CP is violated (otherwise baryons and antibaryons are generated in the same rate) and 3) non equilibrium conditions (since we believe that CPT is conserved, particles and antiparticles have the same mass, and therefore in thermal equilibrium they have the same abundance).

It turns out that within the SM these 3 conditions are never fulfilled. Specific extensions of the SM could generate the observed  $n_B$ . 'Baryogenesis at the electroweak phase transition' can be tested at accelerators, and seems to require a too light Higgs. 'Baryogenesis trough decays of GUT particles' seems to conflict with non-observation of magnetic monopoles. Other possibilities could work, but we do not know how to test them experimentally.

We here focus on 'baryogenesis via leptogenesis'. The SM is extended by adding the heavy right-handed neutrinos, as suggested by see-saw models. Their decays can generate the observed amount of matter,

Their decays generate matter.

$$\Gamma = \frac{\lambda^2}{8\pi} M$$

Matter in decays of

See-saw models right-handed neutrinos. They decay at  $T \sim M$

Sphaleons,  $B - L$  anomaly free.

Formula: An accurate enough approximate formula

$$\frac{n_B}{n_\gamma} \approx 0.01 \eta \epsilon$$

where 0.01 (one over the  $\sim 100$  SM dof)

**inverted hierarchy**  $L_e - L_\mu - L_\tau$ , in see saw charge

Can be SU(5)-unified:



# A Acronyms

$0\nu 2\beta$	Neutrino-less double beta (decay).	MSSM	Minimal Supersymmetric Standard Model
CMB	Cosmic Microwave Background	MSW	Matter corrections to neutrino oscillations
CC	Charged Current: scattering that transforms $\nu$ into charged leptons.	NC	Neutral Current: scattering that does not transform $\nu$ into charged leptons.
CL	Confidence Level	NRO	Non Renormalizable Operator.
CNGS	CERN to Gran Sasso (long baseline experiment).	QVO	Quasi-Vacuum Oscillations: a solution of the solar neutrino anomaly.
dof	degree of freedom	SNO	Sudbury Neutrino Observatory: a solar experiment.
ES	Electron Scattering (of neutrinos).	SK	SuperKamiokande: japanese experiment.
GNO	Gallium Neutrino Observatory: a solar neutrino experiment.	SM	Standard Model of particles
GUT	Grand Unified Theory	SMA	Small Mixing Angle: a solution of the solar neutrino anomaly strongly disfavoured by data.
K2K	KEK to Kamioka (long-baseline experiment).	SSM	Standard Solar Model
LEP	the most recent $e\bar{e}$ collider at CERN.	SUSY	SUperSYmmetry.
LFV	Lepton Flavour Violation	vev	vacuum expectation value
LHC	Large (or Last) Hadron Collider	VO	Vacuum Oscillations: a solution of the solar neutrino anomaly strongly disfavoured by data.
LMA	Large Mixing Angle: a solution of the solar neutrino anomaly	WČ	Water Čerenkov: experimental technique.
LOW	Another solution of the solar neutrino anomaly, also with large mixing angle.		
LSND	A reactor experiment that claims $\bar{\nu}_\mu \rightarrow \bar{\nu}_e$ oscillations.		
MINOS,			

# B Statistics

## References

- [1] E. Fermi, “ *Versuch einer Theorie der  $\beta$ -Strahlen*”, Zeitschrift für Physik XXXXX
- [2] F.J. Botella, C.S. Lim, W.J. Marciano, *Phys. Rev.* D35 (1987) 896.
- [3] First analytical formulae were obtained in S. Parke, *Phys. Rev. Lett.* 57 (1986) 1275; P. Pizzochero, *Phys. Rev.* D36 (1987) 2293. Eq. (17) was found in S.T. Petcov, *Phys. Lett.* B200 (1988) 373. For a review see T.K. Kuo, J. Pantaleone, *Rev. Mod. Phys.* 61 (1989) 937. For recent useful studies of matter effects in the QVO region see G.L. Fogli,



E. Lisi, D. Montanino, A. Palazzo, *Phys. Rev. D* **62** (2000) 113004 (*hep-ph/0005261*); E. Lisi, A. Marrone, D. Montanino, A. Palazzo, S.T. Petcov, *Phys.*

*Rev. D* **63** (2001) 93002 (*hep-ph/0011306*).

[4] G. L. Fogli, E. Lisi and A. Marrone, *Phys. Rev. D* **64** (2001) 093005 [*arXiv:hep-ph/0105139*].